# Sphalerons, baryogenesis, and helical magnetogenesis in the electroweak transition of the minimal standard model

Dmitri Kharzeev,[1,2] Edward Shuryak,[1] and Ismail Zahed[1]

[1]*Department of Physics and Astronomy, Stony Brook University, Stony Brook, New York 11794, USA*
[2]*Physics Department and RIKEN-BNL Research Center, Brookhaven National Laboratory, Upton, New York 11973, USA*

(Received 21 February 2020; accepted 21 September 2020; published 15 October 2020)

We start by considering the production rates of sphalerons with different sizes $\rho$ in the symmetric phase, $T > T_{\rm EW}$. At small $\rho$, the distribution is cut off by the growing mass $M \sim 1/\rho$, and at large $\rho$ by the magnetic screening mass. In the broken phase, $T < T_{\rm EW}$, the scale is set by the Higgs vacuum expectation value $v(T)$. We introduce the concept of "sphaleron freeze-out" whereby the sphaleron production rate matches the Hubble Universe expansion rate. At freeze-out the sphalerons are out of equilibrium. Sphaleron explosions generate sound and even gravity waves, when a nonzero Weinberg angle makes them nonspherical. We evaluate the magnitude of $CP$ violation during the sphaleron explosions. We assess its magnitude using the Standard Model Cabbibo-Kobayashi-Maskawa (CKM) quark matrix, first for nonzero and then zero Dirac eigenstates. We find that its magnitude is maximal at the sphaleron freeze-out condition with $T \approx 130$ GeV. We proceed to estimate the amount of $CP$ violation needed to generate the observed magnitude of baryon asymmetry of the Universe, and find that it is about an order of magnitude above our CKM-based estimates. We also relate the baryon asymmetry to the generation of $U(1)$ magnetic chirality, which is expected to be conserved and perhaps visible in polarized intergalactic magnetic fields.

DOI: 10.1103/PhysRevD.102.073003

## I. INTRODUCTION

One of the central unsolved problems of physics and cosmology is *baryogenesis*, the explanation of the apparent baryon asymmetry (BAU) in the Universe. Since the problem involves many areas of physics, our introduction will be split into several parts for their brief presentation. The common setting is the cosmological electroweak phase transition (EWPT), whereby the universe undergoes a transition from a symmetric phase to a broken phase with a nonzero vacuum expectation value (VEV) for the Higgs field.

Most of the studies of the EWPT, from early works till now, assumed the phase transition to be first order, producing bubbles with large-scale deviations from equilibrium [1]. Most studies of gravitational radiation were carried in this setting. However, Ref. [2] and subsequent lattice studies have shown that the standard model (SM) can only undergo a first order transition for Higgs masses well below the $M_H \approx 125$ GeV mass observed at LHC. The first order transition remains possible only in the models that go beyond the standard model (BSM), which we do not discuss in this work.

Another possible scenario of the EWPT is the "hybrid" or "cold" scenario, suggesting that the broken symmetry phase happens at the end of the inflation epoch. Here, the label "cold" refers to the fact that at the end of the reheating and equilibration of the Universe, the temperature becomes of the order of $T = 30$–$40$ GeV, well below the critical electroweak temperature $T_{\rm EW} \approx 160$ GeV. Violent deviations from equilibrium occur in this scenario [3,4]. Detailed numerical studies [4,5] revealed "hot spots," filled with strong gauge fields, later identified [6] with certain multiquanta bags containing gauge quanta and top quarks. We do not consider this scenario in this work.

Instead, we will focus on the least violent scenario for the EWPT, a smooth crossover transition expected from the minimal Standard Model. The main cosmological parameters of the EWPT are by now well established. For completeness they are briefly summarized in the Appendix A.

Sphaleron transitions are topologically nontrivial large-amplitude fluctuations of the gauge field, resulting in change of their Chern-Simons number $N_{\rm CS}$. Because of the chiral anomaly, in electroweak theory this also leads to changed baryon $B$ and lepton $L$ charges. The introduction to sphalerons is in Sec. II A and technical details (such as the explicit solutions) are in Appendix B.

As noted by Sakharov long ago [7], any mechanism contributing to the BAU needs to include three key components: (1) deviation from equilibrium; (2) baryon number violation; and (3) $CP$ violation.

It is well known that the SM includes all these conditions "in principle." One may expect certain deviations from equilibrium in the expanding Universe, passing through the phase transition. The sphaleron explosions produce $\pm 3$ units of baryon and lepton numbers. The $CP$ violation does happen, due to the well-known complex phase of the Cabbibo-Kobayashi-Maskawa (CKM) quark matrix. However, specific scenarios based on SM were so far unable to reproduce the key observed BAU parameter, the baryon-to-photon ratio

$$\frac{n_B}{n_\gamma} \sim 6 \times 10^{-10}, \tag{1}$$

well documented at the time of primordial nucleosynthesis.

As a result, the mainstream of BAU studies has shifted mostly to scenarios containing unknown physics BSM, in which hypothetical sources of $CP$ violation are introduced (e.g., axion fields, or extended Higgs or neutrino sector with a large $CP$ violation). The so-called *leptogenesis* scenarios use superheavy neutrino decays, occurring at very high scales, and satisfying both large $CP$ and out-of-equilibrium requirements, with large lepton asymmetry transformed into the baryon asymmetry by the electroweak sphalerons at $T_{\rm EW}$. While one of these BSM scenarios may well turn out to be the explanation for BAU, they still remain purely hypothetical at this time, lacking any support from current experiments.

The aim of this work is to provide a scenario *within the SM* that maximizes BAU. We will estimate, as accurately as possible at this time, the magnitude of BAU that the SM predicts. Throughout, we will keep to a conservative and minimal SM (MSM) scenario, in which the EWPT is smooth, with a gradual building of the Higgs VEV $v(T)$ at $T < T_c$. The needed "out-of-equilibrium" conditions to be discussed below, will be associated with "sphaleron freeze-out" of large-size sphalerons, with the rates comparable with the universe expansion rate. Contrary to popular opinion, it turns out to be only an order of magnitude below what is phenomenologically needed. We therefore think that this scenario deserves much more detailed and quantitative studies.

The core of this paper is Sec. III A, in which we discuss $CP$ violation associated with sphaleron explosions. We develop "eigenstate" formalism, generalizing momentum representation used in standard Feynman diagrams. We discuss then $CP$ violation for nonzero and zero eigenvalue sectors subsequently, finding that the latter produces effects of the order of $10^{-9}$. We further show that this estimate leads to BAU much larger than expected before, only about a decade lower than the observed value.

In Sec. VII we discuss other potential observables produced by the sphaleron explosions, namely production of sounds, gravity waves, and helical magnetic fields.

The "sphaleron explosion" is described by a time-dependent solution of the classical Yang-Mills equations. A number of such solutions have been obtained numerically. Analytic solutions for pure-gauge sphalerons have been obtained in [8] and in [9], of which we will use the latter one. Some details of how it was obtained and some basic formulas are summarized in Appendix B.

As we will see below, the word "explosion" is not a metaphor here. Indeed, the time evolution of the stress tensor $T^{\mu\nu}(t,\vec{x})$ does display an expanding shell of energy density and pressure. Although we have not studied its interaction with ambient matter in any detail, it is clear that a significant fraction of the sphaleron mass should end up in spherical sound waves.

In the symmetric phase, the sphaleron explosion is spherically symmetric. It does not sustain a quadrupole deformation and therefore cannot radiate direct gravitational waves. However, the indirect gravitational waves can still be generated at this stage, through the process

$$\text{sound} + \text{sound} \to \text{gravity wave}$$

pointed out in [10]. After the EWPT, at $T < T_{\rm EW}$, the nonzero VEV breaks the symmetry and the sphalerons (and their explosions) are no longer spherically symmetric. With a nonzero and time-dependent quadrupole moment, they generate direct gravitational radiation. We will calculate the corresponding matrix elements of the stress tensor in Sec. VII A.

The EWPT has also been suggested to be a source for large scale magnetic fields in the universe. The existence and properties of intergalactic magnetic fields are hotly debated by observational astronomers, cosmologists, and experimentalists specialized in the detection of very high energy cosmic rays. Currently, there are lower and upper limits on the magnitude of these fields. The issues of the chirality of these fields as well as their correlation scale are still open questions, with suggestions ranging from larger than the visible size of the universe (in case of preinflation chiral fluctuations) to sub-Galaxy size. Many things *may* happen on the way from the big bang to today's magnetic fields.

We discuss the properties of magnetic clouds generated by sphaleron explosions in Sec. VII B. Our main point is that the sphaleron-induced BAU must also be related with the chiral imbalance of quarks and leptons produced in sphaleron transitions. This chiral imbalance is then transferred to linkage of magnetic fields. Since the linkage is expected to be conserved in plasmas, it may be observable today, via the selection of a magnetic helicity in the intergalactic magnetic fields.

## II. SPHALERONS NEAR THE CROSSOVER EW PHASE TRANSITION

### A. Sphaleron, the introduction

The multidimensional effective potential $V(N_{\rm CS})$ possesses a one-parameter sphaleron path, along which thermal fluctuation can cause a slow "climb" uphill, to the saddle points at half-integer $N_{\rm CS}$, the *sphalerons* (e.g., from $N_{\rm CS}=0$ to $N_{\rm CS}=\frac{1}{2}$). The explicit static and purely magnetic gauge configuration was originally found in [11]. When perturbed, the saddle point configuration leads to a classical roll down in the form of a time-dependent solution known as the sphaleron explosion. The Chern-Simons number in such processes changes back from half-integer to integer (e.g., from $N_{\rm CS}=\frac{1}{2}$ to $N_{\rm CS}=1$ or 0).

At low temperatures $T<T_{\rm EW}$, in the symmetry-broken phase, sphalerons have large mass, and the transition rate is strongly suppressed by the corresponding Boltsmann factor. However, in the symmetric (unbroken) phase with $v(T>T_{\rm EW})=0$, the sphaleron rate is only suppressed by the (fifth) power of the coupling [12,13], without exponent $\Gamma/T^4\sim\alpha_{\rm EW}^5\sim 10^{-7}$. In the broken phase after the EWPT with $v(T<T_{\rm EW})\neq 0$, it is suppressed further, by a Boltzmann factor $\exp[-M_{\rm sph}(T)/T]$ with a $T$-dependent sphaleron mass. Some basic information about the electroweak sphaleron rate is given in Appendix B. We start this work by discussing the sphaleron size distribution. This is done separately for (a) unbroken and (b) broken phases [with nonzero Higgs VEV $v(T)\neq 0$].

In case (a) one can ignore the Higgs part of the action and focus on the gauge part. At small sizes the distribution is cut off because the sphaleron mass is increasing $m\sim 1/\rho$ (by dimension), with the pure gauge solution discussed in [8,9]. At large sizes, the limiting factor is the magnetic screening mass which we will extract from lattice data [14]. We then interpolate between the "large size" and "small size" expressions, with the overall normalization of the rate tuned to available lattice data [15].

In case (b) we follow the original work in [11], by inserting the appropriate parameters of the effective electroweak action near $T_{\rm EW}$ calculated in [16]. Specifically, we use a one-parameter Ansatz depending on the parameter $R$, for which both the mass $M(R)$ and the rms size $\rho(R)$ are calculated. The results will be summarized in Fig. 1 below.

### B. The temperature dependence of the sphaleron rates

To assess the temperature of the sphaleron rate, we first start in the symmetric phase with zero Higgs VEV and $T>T_{\rm EW}$. The change in the baryon number is related to the sphaleron rate through [17,18]

$$\frac{1}{N_B}\frac{dN_B}{dt}=\frac{39\Gamma}{4T^3}. \tag{2}$$

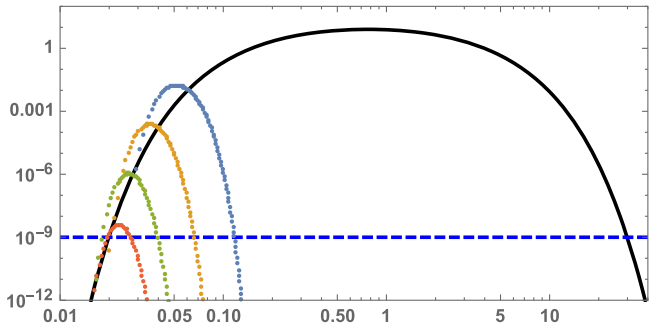


FIG. 1. The sphaleron suppression rates as a function of the sphaleron size $\rho$ in $\mathrm{GeV}^{-1}$. The solid curve corresponds to the unbroken phase $v=0$ at $T=T_{\rm EW}$. Four sets of points, top to bottom, are for a well broken phase, at $T=155$, 150, 140, 130 GeV. They are calculated via Ansatz B described in Appendix C, and normalized to lattice-based rates. The horizontal dashed line indicates the Hubble expansion rate relative to these rates.

The sphaleron rate calculated from earlier lattice studies and also derived from Bodeker model is

$$\Gamma=\kappa\left(\frac{gT}{m_D}\right)^2\alpha_W^5T^4 \tag{3}$$

with $\kappa\sim 50$ extracted from the lattice fit. The lattice work [15] yields a more accurate evaluation for the rate

$$\frac{\Gamma}{T^4}=(18\pm 4)\alpha_{\rm EW}^5\approx 1.5\times 10^{-7}. \tag{4}$$

While (4) appears small, its folding in time at the electroweak transition temperature $T_{\rm EW}$ is large,

$$\frac{1}{N_B}\frac{dN_B}{dt}=3.2\times 10^9\frac{1}{t_{\rm EW}}. \tag{5}$$

Therefore, the baryon production rate in the symmetric phase strongly exceeds the expansion rate of the Universe $H\sim 1/t_{\rm EW}$, by 9 orders of magnitude. Therefore, prior to EWPT, $T\geq T_{\rm EW}$, the sphaleron transitions are in thermal equilibrium. According to Sakharov, this excludes the formation of BAU. In fact, this even suggests a total wash of baryon-lepton (BL) asymmetry. This particular conclusion will be circumvented below, by the sphaleron freeze-out phenomenon.

Another important result of the lattice work [15] is the temperature dependence of the sphaleron rate in the symmetry broken phase

$$\mathrm{Log}\left(\frac{\Gamma(T<T_{\rm EW})}{T^4}\right)=-(147.7\pm 1.9)+(0.83\pm 0.01)\left(\frac{T}{\rm GeV}\right). \tag{6}$$

It would be useful for our subsequent discussion to reparametrize this rate, expressing it in terms of the sphaleron mass through the temperature-dependent Higgs VEV $v(T)$, namely

$$\frac{\Gamma}{T^4}\sim \exp\left(-\frac{\Delta M_v}{T}\right) \tag{7}$$

with

$$\Delta M_v(T)\approx \frac{v(T)^2}{9\ \rm GeV}. \tag{8}$$

By comparing this rate to the Hubble value for the Universe expansion rate at the time $t_{\rm EW}$, the authors of Ref. [15] concluded that the sphaleron transitions become irrelevant when the temperature is below

$$T_{\rm decoupling}=131.7\pm 2.3\ \rm GeV. \tag{9}$$

So, our subsequent discussion is limited to the times when the temperature is in the range

$$T_{\rm EW}\approx 160\ \rm GeV<T<T_{\rm decoupling}\approx 130\ \rm GeV.$$

Note that by this time, the Higgs VEV (A6) reaches only a fraction of its value today, in the fully broken phase, i.e., $v(T=0)\approx 246$ GeV.

### C. The sphaleron size distribution

The lattice results recalled above gave us valuable information of the mean sphaleron rates and thus masses. However, for the purposes of this work, we need to know their size distribution. As we will detail below, baryogenesis driven by $CP$ violation is biased toward sphalerons of sizes larger than average, while the gravity wave signal and seeds of magnetic clouds are biased to smaller sizes.

#### 1. Unbroken phase and small sizes

Let us start with the small-size $\rho$ part of the distribution. In this regime, we can ignore the Higgs VEV, even when it is nonvanishing, a significant simplification. By dimensional argument it is clear that $M_{\rm sph}(\rho)\sim 1/\rho$. It is also clear that small-size sphalerons should be spherically symmetric.

The classical sphaleron-path configurations in pure gauge theory were analytically found in [8]. The method used is "constrained minimization" of the energy, keeping their size $\rho$ and their Chern-Simons number $N_{\rm CS}$ fixed. This gave the explicit shape of the sphaleron barrier. At the highest point of the barrier $N_{\rm CS}=\frac{1}{2}$, the sphaleron mass is

$$M_{\rm sph}(\rho)=\frac{3\pi^2}{g^2\rho}. \tag{10}$$

Later the same solutions were obtained in [9] by a different method, via an off-center conformal transformation of the Euclidean solution (the instanton) of the Yang-Mills equation. Some of the results are reviewed in Appendix B. It provides not only a static sphaleron configuration but also the whole *sphaleron explosion process* in relatively simple analytic form, to be used below.

#### 2. Unbroken phase and large sizes

Now we turn to the opposite limit of large-size sphalerons. Since the sphaleron itself is a magnetic configuration, at large $\rho$ one should consider magnetic screening effects. Unlike the simpler electric screening, the magnetic screening does not appear in perturbation theory [19]. It is purely nonperturbative and likely due to magnetic monopoles.

The magnetic mass $M_m$ conjectured by Polyakov to scale as $M_m=\mathcal{O}(g^2T)$ was confirmed by lattice studies. While in the QCD plasma the coupling is large and the difference between the electric and magnetic masses is only a factor of 2 or so, in the electroweak plasma the coupling is small $\alpha_{\rm EW}\sim 1/30$, and therefore the magnetic screening mass is smaller than the thermal momenta by about 2 orders of magnitude,

$$\frac{M_m}{3T}\sim\frac{\alpha_{\rm EW}}{3}\sim 10^{-2}. \tag{11}$$

The key consequence for the sphalerons is that their sizes would be about 2 orders of magnitude larger than the interparticle distances in the electroweak plasma.

The part of the gauge action related with the screening mass is

$$\Delta S_{\rm screening}=\frac{M_m^2}{2}\int d^4x(A_i^a)^2. \tag{12}$$

For static sphalerons, the integral over the Matsubara time is trivial, giving $1/T$. Parametrically, we have $M_m\sim g^2T$, $A\sim 1/g\rho$, so that

$$M_m^2\int d^4x(A_i^a)^2\sim (g^2T)^2\left(\frac{1}{g\rho}\right)^2\frac{\rho^3}{T}\sim g^2T\rho. \tag{13}$$

At high temperature, the pure SU(2) lattice simulations in [14] give

$$M_m(T) \approx 0.457 g^2 T. \tag{14}$$

Inserting (14) in (12) and using the pure gauge sphaleron configuration yield the screening factor for large size sphalerons

$$\frac{\Gamma}{T^4} \sim \exp(-(0.457)^2 \pi^2 g^2 T \rho). \tag{15}$$

### D. The broken phase not too close to $T_{\rm EW}$

In this case one can follow what has been done in the original sphaleron paper [11], substituting into it appropriate couplings of the effective theory at finite temperature calculated in [16].

We used the so-called Ansatz B, expressing the sphaleron mass $M(R)$ and its rms $\rho(R)$ versus its parameter $R$. Since this material is rather standard, we put the related expressions in the Appendix C. The results will be given in the next subsection.

#### 1. The sphaleron size distribution

We start with the unbroken phase, $T > T_{\rm EW}$. The sphaleron size distribution can now be constructed using the mean mass (8), as well as the small and large size limits (10) and (15). More specifically, the distribution interpolates between the small and large size distributions which merge at $\rho = \rho_{\rm mid} = 0.8$ GeV to give (7)

$$P(\rho, T) \sim \exp\left[-\frac{3\pi^2}{g^2 T}\left(\frac{1}{\rho} - \frac{1}{\rho_{\rm mid}}\right)\right] \times \exp[-(0.457)^2 \pi^2 g^2 T(\rho - \rho_{\rm mid})]. \tag{16}$$

In Fig. 1 we show the sphaleron size distribution at the critical temperature (the solid line) and four temperatures below it, in the broken phase. We see that the appearance of a nonzero Higgs VEV leads not only to a suppression of the rate, but also to a dramatic decrease of the sphaleron sizes. The lowest temperature shown, $T_L \approx 130$ GeV, corresponds to the sphaleron rate that reaches the Universe expansion rate (Hubble).

The intercept of each curve with the dashed horizontal line gives (the smallest and) the largest size sphalerons which have rates comparable to the Universe expansion rate, and should therefore be "at freeze-out," out of thermal equilibrium. One can see that for four sets of points shown, $\rho_{\rm max}$ changes from about $1/(10\ {\rm GeV})$ to $1/(30\ {\rm GeV})$. Very close to the critical temperature $T_{\rm EW}$ the sphalerons may be significantly larger in size, as seen from a comparison to the black curve. However, the related uncertainty does not matter, as we will show below, because in this region the $CP$ asymmetry is extremely small, growing toward $T = 130$ GeV.

## III. $CP$ VIOLATION AND THE SPHALERON EXPLOSIONS

### A. Introductory discussion of $CP$ violation induced by the CKM matrix

In this section we discuss whether the "minimal" $CP$ violation in the SM, following from the experimentally well studied complex contribution of the CKM matrix, can generate the required level of asymmetry. Needless to say, this question was addressed by many in talks and textbooks, but it is worth reviewing it again here.

The $CP$ violation in the SM is induced by the nonzero phase of the CKM matrix. Its magnitude is known to be strongly scale dependent. Naively, at $T_{\rm EW}$ all particle momenta are of the order of $p \sim 3T \sim 500$ GeV, above all quark masses. As originally shown by Jarlskog [20], at such a high scale the magnitude of the $CP$ violation needs to be proportional to the product of two different factors. The first is the so-called "Jarlskog determinant" $J$ containing the sine of the $CP$-violating phase $\sin(\delta)$ times sines and cosines of the mixing angles. $J$ has a geometric meaning, so it is invariant under reparametrization of the CKM matrix. Its numerical value is $J \sim 3 \times 10^{-5}$. The second factor is the (dimension 12) product of the string of squared up and down quark mass differences

$$\Delta \equiv (m_b^2 - m_d^2)(m_b^2 - m_s^2)(m_d^2 - m_s^2) \times (m_c^2 - m_t^2)(m_c^2 - m_u^2)(m_t^2 - m_u^2), \tag{17}$$

which ensures that $CP$ asymmetry vanishes whenever any two masses of up-kind or down-kind quarks are equal. The resulting $CP$ asymmetry at electroweak momentum scale $p \sim \pi T$ is very small, $A_{CP} \sim J \cdot \Delta / p^{12} \sim 10^{-21}$ [21], which seemingly dash any hopes that the SM $CP$ violation may significantly contribute to BAU. Explicit perturbative calculations of the $CP$-violating parts of the effective Lagrangian at finite temperatures [22] also show that at temperatures $T \sim 130$ GeV we discuss the overall $CP$ violation magnitude is negligibly small.

However, such calculations cannot be directly applied to sphalerons and their explosions, because their fields are strong $W_\mu(x) \sim 1/g$ and one cannot use perturbative expansion in their power. We therefore use an eigenstate formalism, using as a basis set of eigenstates of the simplified Dirac operator, for unmixed massless fermions. The CKM mixing and fermion masses are treated explicitly. If so, the integration over intermediate momenta in the Feynman diagrams changes to sums over eigenvalues $\lambda$.

The distribution over $\lambda$ has two parts, (i) the *nonzero* spectrum; and (ii) the topological zero mode $\lambda = 0$. We estimate below the corresponding $CP$ violation in these two sectors, subsequently.

For the sector with nonzero $\lambda$ our calculation of the $CP$-violating effects shows a dramatic dependence on $\lambda$ (shown in Fig. 3). In agreement with Smit's arguments [23], there is no effect in the fourth order in CKM mixing alone, and it appears only, e.g., when two powers of a $Z$ field are involved. We also find that the $CP$ violation can be as large as $\sim J \sim 10^{-5}$ for $\lambda \sim 1$ GeV, in a "sweet spot" between the masses of the light and heavy quarks. However, gluon scattering on quarks shifts the lowest $\lambda$ to the so-called Klimov-Weldon mass: the result of that would be a small $CP$ violation comparable to the old Shaposhnikov's estimate [21].

Before discussing our (quite different) results from our estimates of the $CP$ violation associated with the zero mode, let us mention the key point. The zero mode is of *topological origin*, it is related with the chiral anomaly, and it describes the states of quarks *produced* out of vacuum by the sphaleron field.

While the background of a sphaleron explosion is analytically known only for some restricted setting (zero temperature and zero Higgs VEV), a generic argument of the *topological stability* tells us that the Dirac zero mode (and the baryon number violation with it) should be preserved also in the presence of finite-$T$ plasma perturbations (such as quark scattering off thermal gluons). In this respect, the zero Dirac eigenmode is different from "small momenta" scenarios associated with them, such as [24].

Let us add at this point that a strict relation between the Chern-Simons number and the baryon charge has been demonstrated in lattice study [25]. While short of calculating the Dirac eigenvalue spectrum and explicitly observing the zero mode in any configurations describing sphaleron transitions, it, however, will display the topological stability of the basic mechanism, based on the chiral anomaly.

We estimate the magnitude of the $CP$ violation at a generic zero Dirac eigenvalue from the (flavor-dependent) phases of the outgoing quark waves (the zero mode itself). We do it for production of different quark types separately, and for light $u$ and $d$ quarks we found it to be of magnitude $10^{-9}$.

It is important to note at this point that while our results contain *some* differences of squared masses of quarks, they do not include the full product of the string of *all* mass differences $\Delta$ (17). This leads to a debate whether such answers can be correct, and therefore we repeat here that it need *not* be universally present in *any* $CP$-violating process. (Indeed, if this is the case we would never know about $CP$ violation since one would not be able to observe it experimentally.)

Let us give example in which it is seen explicitly. The $CP$ violation originally discovered in neutral $K$ decays is of magnitude $\sim 10^{-3}$, but these processes are complicated by the relation to the $K^0 - \bar{K}^0$ mass difference. Consider a much simpler example, a "direct $CP$ violation" in *exclusive* charged meson (or baryon) decays, induced by reactions of the type $b \to \bar{q}qq'$ (e.g., $b \to \bar{c}cs$) or many others. The tree diagram of the decay has two CKM matrix elements, and $CP$ violation comes from the interference with the so-called "penguin" diagrams, with an additional gluon, producing a $\bar{q}q$ pair. This second diagram has in general a sum over up-type quarks $U = u,\ c,\ t$ and therefore CKM matrix elements $V_{bU}$ and $V_{Uq'}$. $CP$ asymmetry of such decays is not only observed, but is rather large, suppressed only by the strong coupling constant and some numerical smallness of a loop, such as $1/4\pi$.

Our point here is based on the following observation: out of three generation of down quarks, only two (say, $b$, $s$) are involved, while the remaining one (say, $d$) is *not*. Therefore, an expression for $CP$ asymmetry cannot possibly contain $m_d$, and therefore factors $(m_b^2 - m_d^2)(m_s^2 - m_d^2)$ cannot be there. The presence of the $\Delta$ factor is not really a universal feature of $CP$ violation; in particular, it is not the case in certain exclusive processes.

(We do know that in the Universe with, say, $m_d = m_s$, there should be no $CP$ violation. It happens as follows: when $|m_d - m_s|$ gets very small, a hadronic spectrum would be rearranged so that $CP$-violating amplitudes for some exclusive processes would need to be added together, partially canceling each other and restoring the $|m_d - m_s|$ in the appropriate kinematical region.)

### B. *CP*-violating perturbative effective action

While the sphaleron decay process has been discussed at the classical level (see Appendix B), the $CP$-violating effects appear at the one-loop level with the contribution from all generations of quarks and their interferences. We are not aware of any consistent calculation of the corresponding $CP$ violation during the sphaleron decays.

The determinant of the Dirac operator in such field $\mathrm{Log}(\det(\hat{D}))$ generates the effective action, induced by the one-loop fermion process, which is similar to the well-known Heisenberg-Euler effective action in QED, with the $CP$-violating part extracted from its imaginary part.

The resulting operators in effective Lagrangian are classified by a two-integer $m + n$ form, with $m$ being the power of the $W$ fields and $n$ the combined power of derivatives, $Z$ and Higgs $\phi$ fields. Studies along these perturbative lines were started by Smit [23] who found that the lowest $4 + 0$ order operators produce *no* $CP$ violation. The calculation in [26] reported a nonzero contribution to order $(4 + 2)$ from the following dimension-six $P$-odd and $C$-even operator:

$$\epsilon^{\mu\nu\lambda\sigma}(Z_\mu W^+_{\nu\lambda} W^-_\alpha (W^+_\sigma W^-_\alpha + W^+_\alpha W^-_\sigma) + \text{c.c.}). \quad (18)$$

Another group [27], however, found a different set of $(4+2)$ operators, which are $C$-odd and $P$-even. This calculation has been extended to nonzero temperature and $6+2$ operators in [22]. The corresponding coefficients are complicated functions of all quark masses, the temperature, and the Higgs VEV.

It is not a trivial task to find an example of the field which would give a nonvanishing expectation value for these operators. In particular, it should be $T$-odd, and thus involve time evolution or electric field strength: therefore sphalerons themselves would not contribute, only their explosions. We have checked using the analytic solution for the sphaleron explosion [8,9] described in Appendix B that it does give a nonvanishing expectation value for the operator (18). It would be interesting to check if this is also the case for other $4+2$, $6+2$ operators identified in [22,27].

### C. Diagrams in eigenstate formalism

The effective action described above is perturbative, obtained from an expansion in powers of electroweak coupling and field $gW_\mu$. This approach is, generally speaking, inapplicable for nonperturbative fields (instantons, sphalerons, etc.), for which $gW_\mu \sim O(1)$ and all terms of a perturbative series are of the same magnitude. Yet there is an effective one-loop effective action, $S_{\text{eff}} = \log\ \det(\not{D})$ of the Dirac operator, the slash here and below means the convolution with the Dirac matrices $\gamma_\mu$.

Using left-right spinor notations, this operator has the matrix form

$$\det\begin{pmatrix} i\not{D} & M \\ M^\dagger & i\not{\partial} \end{pmatrix} = \det(i\not{\partial})\det\left(i\not{D} + M\frac{1}{i\not{\partial}}M^\dagger\right), \quad (19)$$

where the interaction with the electroweak gauge fields $W$, $Z$ is in left-left sector, the mass-generating interactions with Higgs have left-right and right-left structure, and the right-right sector is free. Recall that $M$ is a (diagonal) mass matrix in flavor space.

The left-left part can be written in the form

$$i\not{D} = (i\partial_\mu + gW_\mu + gZ_\mu)\hat{1}\gamma_\mu + gW_\mu(\hat{V}-\hat{1})\gamma_\mu, \quad (20)$$

where a hat indicates flavor matrices, with $\hat{V}$ being a (weakly nondiagonal) CKM matrix. Let us then introduce eigenstates of the operator in the former bracket

$$(i\partial_\mu + gW_\mu + gZ_\mu)\hat{1}\gamma_\mu\psi_\lambda(x) = \lambda\psi_\lambda(x), \quad (21)$$

which treats all quarks as universal (flavor diagonal) massless objects. (Therefore this part of the Dirac operator remains conformal, and its zero mode can thus be analytically obtained using conformal off-center transformation from the instanton, as described in Appendix B.)

The remaining part of the Dirac operator can be treated perturbatively, formally using $(\hat{V}-\hat{1})$ as a small parameter. This setting leads to close loop Feynman diagrams, in which propagators can be represented by the sum over modes

$$S(x,y) = \sum_\lambda \frac{\psi^*_\lambda(y)\psi_\lambda(x)}{\lambda + M\not{p}^{-1}M^+} \quad (22)$$

and vertices containing flavor matrices $(\hat{V}-\hat{1})$ and the matrix element of two modes of the current times the gamma matrix and the field $\langle\lambda|\not{W}|\lambda'\rangle$. In such a representation one needs to sum over $\lambda$'s in each propagator, as momenta in the usual free field diagrams.

In order to simplify the discussion as much as possible, we defer consideration of the eigenvalue spectrum and summations involved for later, assuming first that we single out *one* particular mode with a particular value of $\lambda$. Let us also focus for now only on diagonal matrix elements, and use shorthand notation

$$\langle\lambda|i\not{\partial}|\lambda\rangle = \not{p}_{\lambda\lambda}, \qquad \langle\lambda|\not{W}|\lambda\rangle = \not{W}_{\lambda\lambda}. \quad (23)$$

Furthermore, we will focus on flavor traces, thus indicating *up* and *down* propagators in a form

$$S_u = \frac{1}{\lambda + M_u^2/\not{p}_{\lambda\lambda}}, \qquad S_d = \frac{1}{\lambda + M_d^2/\not{p}_{\lambda\lambda}}, \quad (24)$$

where we notice that $W$ vertices alternate between up and down flavors. For example, the generic four-$W$ diagram (0) in Fig. 2 takes the form

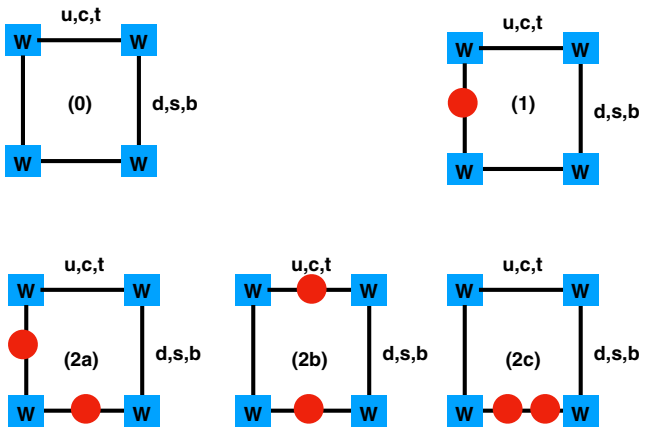


FIG. 2. Schematic description of the fourth order one-quark-loop diagrams with four-$W$ boson insertions shown in blue squares. The additional $Z_\mu$ and $A_\mu$ fields [diagram (0)], one (1), and two ($2a$, $2b$, $2c$) are shown in red circles.

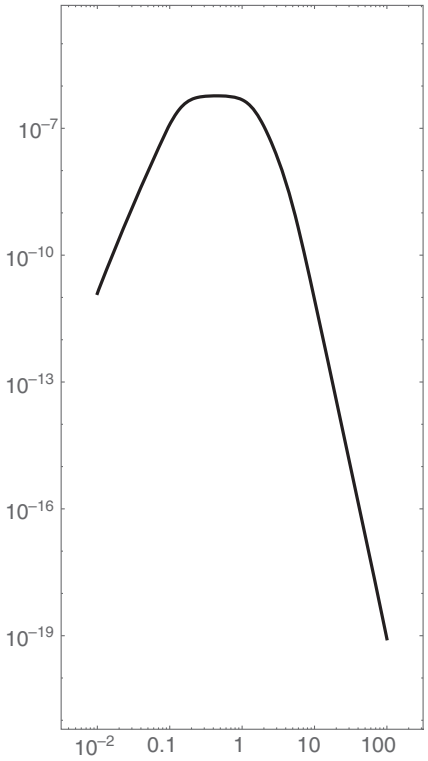


FIG. 3. $CP$-violating contribution $\mathrm{Im}F_{ZZ}(\lambda)$ from diagram (2a) of Fig. 2 versus $\lambda$ (GeV).

$$\mathrm{Tr}(\not{W}_{\lambda\lambda}\hat{V}\hat{S}_u\not{W}_{\lambda\lambda}\hat{V}^\dagger\hat{S}_d\not{W}_{\lambda\lambda}\hat{V}\hat{S}_u\not{W}_{\lambda\lambda}\hat{V}^\dagger\hat{S}_d).$$

It is now straightforward to perform the multiplication of these flavor CKM matrices and propagators with six known quark masses, for all five diagrams shown in Fig. 3, including lowest order insertions of flavor-neutral $Z$ and/or electromagnetic $A^{em}$ fields, shown in Fig. 2 by red circles. The electromagnetic field insertions obviously carry quark electric charges, $e_u = 2/3$ and $e_d = -1/3$.

The explicit flavor traces for these higher order diagrams show that (1, 2b, 2c) do not lead to $CP$-violating $O(\delta)$ terms in the resulting effective Lagrangian also. The only one that does is diagram (2a), with the result

$$\begin{aligned}\mathrm{Im}F_{ZZ}(\lambda) &= \lambda^6\mathrm{ImTr}(\hat{V}S_d\hat{V}^\dagger S_u\hat{V}S_dZS_d\hat{V}^\dagger S_uZS_u)\\ &= \frac{J\Delta 2\lambda^6}{\Pi_{f=1..6}(\lambda^2+m_f^2)^2}.\end{aligned} \tag{25}$$

We recall that $J$ is the famed Jarlskog combination of the CKM cos and sin of all angles times the sin of the $CP$-violating phase, and $\Delta$ is a product of quark squared mass differences (17). Diagram (2a) with 2-$Z$ and 2-$A^{em}$ would then carry an obvious prefactor

$$C_{2a} = \left((Z_\lambda)^2 - \frac{2}{9}(A^{em}_\lambda))^2\right). \tag{26}$$

Since these two terms have opposite signs, no universal statement about the *sign* of the $CP$ violation in an arbitrary background can be made.

In Fig. 3 we show (25) as a function of the eigenvalue scale $\lambda$. It is clear that the magnitude of the $CP$ violation depends on the absolute scale very strongly. When the momentum scale is at the electroweak value $\sim$100 GeV (the right-hand side of the plot), it is $10^{-19}$. But in the "sweet spot," between the masses of the light and heavy quark $\lambda \in (0.2\text{–}2)$ GeV, the asymmetry is suppressed only by about $\sim 10^{-6}$.

## IV. EIGENVALUES AND PLASMA EFFECTS

In the preceding section we discussed a generic part of the effective $CP$-violating Lagrangian related with Dirac eigenvalue $\lambda$. The lesson we learned is that $CP$ asymmetry is strongest if $\lambda \sim 1$ GeV. Now we will face the question of whether such eigenvalues are, in fact, present in the realistic eigenvalue spectral function.

The sphalerons and their explosions have so far been considered classically, via appropriate solutions of the Yang-Mills (and Dirac) equations. The most symmetric case [9] (see Appendix B) corresponds to symmetric phase $T > T_{\mathrm{EW}}$ in which there is no Higgs VEV and the gauge fields are only the $SU(2)$ ones, without electromagnetic ones. In such a setting, the only dimensional parameter, on which the $\lambda$ spectrum may depend, is given by the sphaleron size $\rho$, defining the field strength $E$, $B \sim 1/g\rho^2$. That is why we started by studying the sphaleron size distributions. It is indeed found that, very close to $T_{\mathrm{EW}}$, the sphalerons can be rather large, with fields in the sweet spot $B \sim 1$ GeV$^2$ range, with very favorable $CP$ magnitude.

However, the actual sphaleron explosions happen in a primordial plasma. In the primordial plasma, fermions are modified by their interactions with the thermal medium. While leptons have electroweak interactions only, quarks interact strongly with ambient gluons, with a much stronger coupling constant $g_s$.

A generic argument is that the gauge fields are classical $W, Z \sim O(1/g_{\mathrm{EW}})$ while thermal fields of the plasma are $\sim O(g^0_{\mathrm{EW}})$, so in the leading order they are not modified. However, since we consider sphalerons of different sizes, there appears a parameter $\rho T$. On top of it, thermal fields have a large number of degrees of freedom, so the corrections to a classical approximation needs to be studied.

The issue gets more urgent at the level of the one-loop quark-induced action we use in studies of $CP$ violation. Quark fields, unlike gauge ones, are not classical. The eigenmodes we consider are all normalized to a unit value. Plasma-induced polarization (quark mass) operators come not only from weak interactions but also from thermal gluons. Therefore the formal suppression parameter is $\sim\alpha_s$, which is not so small. A full inclusion of all Dirac modes

following a sphaleron explosion *in a plasma* is still beyond the scope of this work. In this section we provide a qualitative discussion and estimates.

### A. Electric screening

Let us recall the argument put forth at the beginning of Sec. II D 1: since the sphalerons are *magnetic* objects, they can be as large as allowed by the *magnetic* screening mass,

$$\rho \leq \frac{1}{M_m} \sim \frac{1}{g^2 T}.$$

Thus, it can differ from the basic thermal scale $T$ by about 2 orders of magnitude. However, a sphaleron explosion generates an (electroweak) *electric* field as well. Originally directed radially, it accelerates quarks and leptons from their initial state as zero modes to their positive and physical energy final states, violating baryon and lepton numbers. In the final stage, only the transverse electric fields remain, producing physical $W$ and $Z$ that are transversely polarized to the radial direction. We recall that under these conditions all particles are massless or have small masses, as the Higgs VEV is zero or small.

The electric screening mass is $M_E \sim gT$, so the screening length is about $g$ times shorter than the magnetic screening length. The "plasma on-shell masses" of $W$ and $Z$ are also $M_{W,Z} \sim gT$. Both effects are incorporated by an additional thermal contribution to the effective Lagrangian (in momentum representation)

$$\Delta L_{\text{plasma}} = \frac{1}{2}\Pi_{\mu\nu}(T, k_\sigma) A^\mu(k_\sigma) A^\nu(k_\sigma) \tag{27}$$

with the one-loop polarization operator $\Pi$ calculated already in Ref. [28]. So, what qualitative modification can these electric thermal effects produce?

Classically, the sphaleron explosion produces $W$ and $Z$ with momenta $p \sim 1/\rho$, and their total number is of the order of the action $N_{W<Z} \sim 1/g^2 \sim 100$. In the thermal plasma this is no longer possible. The available energy is not sufficient to produce that many gauge quanta since their thermal masses are $M_{W,Z} \sim gT$. Furthermore, at the momenta $p \sim 1/\rho$ corresponding to the initial sphaleron sizes, the plasma modes are not $W$, $Z$ plasmons but rather collective modes of hydrodynamical origin, corresponding to the longitudinal sounds (phonons) and transverse (rotational and purely diffusive) motions. (How exactly the energy is divided between those modes we have not assessed yet: it may be needed for gravity wave predictions.)

As we already noted earlier, due to the nonzero Weinberg angle, some part of sphaleron energy goes to QED electromagnetic fields and eventually to polarized magnetic clouds. Their polarization tensor includes not the electroweak but the electric coupling constant, which is smaller, and so their interaction with the plasma can probably be neglected, once they are produced.

The quark modes acquire larger plasma-induced masses, and one may wonder if those can prevent the $B$, $L$ number violation phenomenon itself.

At this point, a historical comment may be made. When Farrar and Shaposhnikov [24] realized that the $CP$ violation induced by the CKM matrix have the sweet spot mentioned above, they focused on the dynamics of the quarks with *small momenta* $p \sim 1$ GeV $\ll T$. Specifically, they argued that under certain conditions the strange quarks are totally reflected from the boundary of the bubble (they assumed the transition to be first order), while the up/down quarks are not. This scenario has been later criticized, based on higher order corrections to the quark dispersion curves, and the conclusions in [24] have been refuted. For pedagogical reasons, let us split the refuting arguments into three, reflecting on their increased sophistication.

*The first argument* says that the Euclidean thermal formulation with antiperiodic fermionic boundary conditions implies that the minimal fermionic energies are set by the lowest Matsubara mode

$$\omega_M = \pi T \sim 300 \text{ GeV}. \tag{28}$$

Indeed, the typical fermionic momenta are of this order, and the CKM-induced $CP$ violation at this scale is $\sim 10^{-19}$ as we detailed above.

*The second argument* is based on the emergence of a "thermal Klimov-Weldon" quark mass

$$M_{\text{KW}} = \frac{g_s T}{\sqrt{6}} \sim 50 \text{ GeV} \tag{29}$$

induced by the real part of the forward scattering amplitude of a gluon on a quark.

Both arguments were essentially rejected by Farrar and Shaposhnikov, who pointed to the fact that while both effects are indeed there, there are still quarks with small momenta $p \ll T, M_q$ in the Dirac spectrum.

*The third argument*, which is stronger, was given in [29,30]. It is based on the *decoherence* suffered by a quark while traveling in a thermal plasma, as caused by the imaginary part of the forward scattering amplitude (related by unitarity to the cross section of *nonforward* scatterings on gluons). Basically, they argued that if a quark starts with a small momentum, it will not be able to keep it small for a necessarily long time, due to such scattering. The imaginary part is about

$$\text{Im}(M_q) \sim \alpha_s T \sim 20 \text{ GeV}. \tag{30}$$

We now return to the sphaleron explosions we have presented, and ask how such plasma effects can affect their quark production. The most obvious question is that of "insufficient energy." Indeed, if each quark carries a "thermal Klimov-Weldon mass" as the smallest energy at small momenta, is there even enough energy to produce the

expected nine quarks? Altogether, these nine masses amount to about 450 GeV, which is comparable to the total sphaleron mass (10) at a size $\rho \sim 1$ GeV$^{-1}$. Therefore, the classical treatment used above, in which the back-reaction of the quarks on the explosion were neglected, by solving the Dirac equation in a background field approximation, should be significantly modified.

However, there is a simple way around the "insufficient energy" argument. In thermal field theory the sign of the imaginary part of the effective quark mass operator can be both positive or negative. This corresponds to the fact that instead of producing new quarks, the sphaleron amplitude can instead *absorb* thermal *antiquarks* from the plasma.

Still we would argue that, unlike the Farrar-Shaposhnikov scenario [24], our sphaleron-induced baryon number violation should survive all plasma effects. We do not classify quarks by their momenta, but rather by the virtualities or *eigenvalues* of the Dirac operator $\lambda$, in the background of a sphaleron explosion solution.

It is true that the plasma effect will modify the spectral density $P(\lambda)$ in a way that most of the virtualities $\lambda$ are equal to or larger than the thermal Klimov-Weldon mass (29)

$$|\lambda| > M_{\rm KW}.$$

According to Fig. 3, this puts the $CP$ asymmetry to be of order $\sim 10^{-17}$, way too small for BAU.

### B. Fermion zero modes and "topological stability" of $B$, $L$ number violations

A sphaleron explosion is a phenomenon in which the *gauge topology* of the background field is changing. The topological theorems require the existence of a topological *zero mode* of the Dirac operator in the spectral density, $P(\lambda) \sim \delta(\lambda)$. For the analytic form of a sphaleron explosion, discussed in Appendix B, it was explicitly found in Ref. [9]. The same technique, an *off-center conformal transformation* of the $O(4)$ symmetric Euclidean instanton solution, applied to instanton zero mode, leads to Minkowski zero mode, which provides a detailed description of the wave function of outgoing fermions.

Although no explicit solution is known in the background of thermal gluon plasma, we argue that *no plasma effects can negate the existence of the zero mode*, which is robust and *immune to any perturbations* of the sphaleron fields, provided those do not change their *topology*. Indeed, the sphaleron explosion implies changing the Chern-Simons number of the gauge configuration, which is locked to the change in the quark and lepton numbers by the chiral anomaly.

For a skeptical reader, let us provide an example from practical lattice gauge theory simulations, which may perhaps be convincing. At a temperature at and above the critical $T > T_c$, in a quark-gluon plasma (QGP) phase, there are plenty of thermal gluons. And yet, when a configuration with the topological charge $Q = \pm 1$ is identified on the lattice, an exact Dirac eigenvalue with $\lambda = 0$ is observed, within the numerical accuracy, typically $10^{-9}$ or better. Also, the spatial shape of this eigenvalue is in very good agreement with that calculated using semi-classical instanton-dyons [31]. Zillions of thermal gluons apparently have no visible effect on the shape of these modes, in spite of the fact that the gauge fields themselves are undoubtedly strongly modified. Of course, this example is in a Euclidean time setting, while the sphaleron explosion is in a Minkowskian time setting. Real time simulations are much more costly and have only been done, with fermions, in a few works, such as [25]. However, it is beyond doubt that the baryon number violation phenomenon, by itself, is topologically robust and immune to thermal modifications.

## V. $CP$ VIOLATION FOR OUTGOING QUARKS

Now that we argued that the Dirac operator should still have an exact zero mode for a sphaleron explosion, even in the plasma, we now further ask how its presence in the Dirac operator determinant can affect the estimates of the $CP$ violation we made earlier.

Let us return to the Dirac operator (19), in left-right notations, adding effects of quark-gluon scattering. Interaction with gluons, represented by the Klimov-Weldon mass (or more generally, the forward scattering amplitude at an appropriate momentum) should be added to both (left-left) and (right-right) parts of the Dirac operator

$$\det\left(i\not{D} + M_{\rm KW} + M_{\rm LR}\frac{1}{i\not{\partial} + M_{\rm KW}}M^{\dagger}_{\rm RL}\right).$$

Note that the nondiagonal fermion masses (LR and RL) flipping chirality can only come from interaction with the Higgs scalar field, violating chiral symmetry. When there is no Higgs VEV (at $T > T_c$), to lowest order the last term is absent. At the next order, it is proportional to the corresponding Yukawa couplings for different fermion species.

What we argued above means that the plasma-deformed first LL operator $i\not{D} + M_{\rm KW}$ should, as the vacuum version, have a zero eigenvalue. For that, we write

$$i\not{D} = (i\not{\partial} + gA_\mu)\hat{1} + gA_\mu(\hat{M}_{\rm CKM} - \hat{1}), \tag{31}$$

where hats indicate matrices in quark flavors. The topological zero mode $\lambda = 0$ follows from the flavor-diagonal part, as a zero eigenvalue of the first bracket

$$(i\not{\partial} + gA_\mu\hat{1})\psi_\lambda = \lambda\psi_\lambda. \tag{32}$$

The so-called "topological stability" implies that the zero eigenvalue *does not* have any perturbative corrections.

The remaining part of the Dirac operator (31) can formally be considered small and thus treated

perturbatively, providing a small modification of the known explicit solution to the Dirac equation in the background of sphaleron explosion. The deviation of the gauge field term from $\hat{1}$ through

$$gA_\mu(\hat{V}_{\rm CKM}-\hat{1})$$

would provide vertices for flavor changing quarks, and the mass term, in the form

$$M_{\rm LR}\frac{1}{i\partial\!\!\!/+M_{\rm KW}}M^\dagger_{\rm RL},$$

would provide perturbative corrections to the quark propagators connecting these vertices. As we will see, this flavor-dependent part is key for evaluating the magnitude of $CP$ violation.

As explained by 't Hooft long ago [32], the physical meaning of the zero mode of the instanton (or its analytic continuation to Minkowski time [9] we imply here) is the wave function of the outgoing fermion produced. The $CP$ violation induced by the quarks "on their way out" appear due to interferences of certain diagrams with different intermediate states. As a result of that, the production probabilities of quarks and antiquarks are *not* equal. The method to calculate the effect was previously developed by Burnier and one of us [33].

Consider an outgoing quark, accelerated by the electric field of the sphaleron explosion, and interacting on its way with the $W$ field times $\hat{V}_{\rm CKM}-1$ *twice*. The full probability for the quark production contains sums over all possible intermediate flavor states. For example, if the quark started as the $b$ quark, then one has a triple sum over intermediate flavors

$$P_b=\sum_{IJK}(A(b\to I=t,c,u\to J=b,s,d)\times A(J=b,s,d\leftarrow K=t,c,u\leftarrow b)). \tag{33}$$

We now note the three key features of this expression:

(i) the intermediate up quarks $t$, $c$, $u$ in each amplitude need not be the same. The interference of multiple paths in flavor space, induced by the CKM matrix angles, may lead to $CP$ violation.

(ii) the total number of CKM matrices $\hat{V}_{\rm CKM}$ is four, which is just enough to make this $CP$-violating contribution nonzero.

(iii) the combination $\hat{V}^+_{\rm CKM}\hat{V}_{\rm CKM}\hat{V}^+_{\rm CKM}\hat{V}_{\rm CKM}$ and its complex conjugate is not the same as for the corresponding ($\bar{b}$) antiquark.

In light of this, the probability to produce a quark and an antiquark are not equal, i.e., $AA_q\neq\overline{AA_q}$. More specifically, let us write the convolution for a particular initial up-quark state labeled as $U0$,

$$\begin{aligned}AA_{U0}\sim&\sum_{D1,U,D2}{\rm Tr}(\hat{P}_{U0}W(x_1)\hat{V}_{\rm CKM}S^{D1,D1}(x_1,x_2)\\&\times W(x_2)\hat{V}^+_{\rm CKM}\tilde{S}^{U1,U1}(x_2,x_3)W(x_3)\hat{V}_{\rm CKM}S^{D2,D2}(x_3,x_4)W(x_4)\hat{V}^+_{\rm CKM}\hat{P}_{U0}),\end{aligned} \tag{34}$$

where $\hat{V}_{\rm CKM}$ is a $3\times3$ CKM matrix (indices not shown) and $P_{U0}$ at both ends are projectors onto the original quark type. The propagators $S(x,y)$ are diagonal flavor matrices with their indices shown. There are three options for each index, $D1$, $D2=b$, $s$, $d$, and $U0$, $U1=t$, $c$, $u$, so for each quark the probability has $3^3=27$ interfering terms. The intermediate propagator $\tilde{S}^{U1,U1}$ has a tilde, which indicates that it should include the propagation from point $x_3$ to infinity and its conjugate propagation from infinity to point $x_4$. Therefore, its additional phase depends on the distance between these points. The corresponding amplitudes for the antiquarks involve complex conjugate (not Hermitian conjugate) CKM matrices relative to the quark amplitude, namely,

$$\begin{aligned}\overline{AA}_{U0}\sim&\sum_{D1,U,D2}Tr\hat{P}_{U0}W(x_1)\hat{V}^*_{\rm CKM}S^{D1,D1}(x_1,x_2)\\&\times W(x_2)\hat{V}^T_{\rm CKM}\tilde{S}^{U1,U1}(x_2,x_3)W(x_3)\hat{V}^*_{\rm CKM}S^{D2,D2}(x_3,x_4)W(x_4)\hat{V}^T_{\rm CKM}\hat{P}_{U0}.\end{aligned} \tag{35}$$

The difference in the probability of production of a quark and antiquark is denoted by

$$\Delta P_Q\equiv{\rm Im}(AA_Q-\overline{AA}_Q).$$

We now note the following:

(i) the propagators of quarks of different flavors between the same relative points have different phases;

(ii) the locations in the amplitude $x_{1,2}$ need not be the same as the locations $x_{3,4}$ in the conjugate amplitude, so in principle we need to integrate over all of these locations independently.

For a qualitative estimate of (34) and (35) we write the nontrivial flavor-dependent phases in the propagators as

$$S^{QQ} = e^{i\phi_Q},$$

suppressing for an estimate their dependence on the coordinates, and perform the sums with $U0$ referring to all six initial types of quarks. The lengthy result is given in Appendix C. As already indicated, these phases come from the last term in the Dirac operator. Apart from the common phase induced by the $\not{p}$ in it, there are flavor-dependent phases induced by the last term in the Dirac operator

$$\phi_Q = \frac{m_Q^2|x_1 - x_2|}{M_{\rm KW}}. \tag{36}$$

Using for the coordinate distance traveled the sphaleron size (maximal at freeze-out line)

$$|x_1 - x_2| \approx \rho_{\rm max} \sim 1/10\text{–}1/30\ {\rm GeV}^{-1},$$

we introduce a new (temperature-dependent) mass scale

$$M_\rho \equiv \left(\frac{M_{\rm KW}}{\rho_{\rm max}(T)}\right)^{1/2} \sim 40\ {\rm GeV}. \tag{37}$$

Using this notation, the additional phases are just a ratio of (flavor and temperature-dependent) quark mass to $M_\rho$, squared:

$$\phi_Q = \frac{m_Q^2}{M_\rho^2}. \tag{38}$$

When the quark masses are smaller than $M_\rho$, the corresponding phases are small.

Let us now recall that we are discussing the Universe at temperatures across the electroweak transition, with the Higgs VEV $v(T)$ emerging from zero to eventually its value in the broken phase as we have it today. For a specific expression see the lattice result (A6). All quark masses grow in proportions to the VEV, and therefore the ensuing $CP$ violation grows. We will divide this stage of the evolution into two substages.

*Stage 1:* In the quark production probabilities, the four vertices with CKM matrices are connected by three propagators, leading to expressions cubic in $\phi_Q \sim (m_Q/M_\rho)^2$, after expanding the expressions in Appendix C. The end of stage 1 happens when the largest of the phases, that due to the top quark, reaches $O(1)$, or

$$m_t \approx M_\rho \sim 40\ {\rm GeV}. \tag{39}$$

At this time all other quark masses are much smaller than the top quark mass, respective to their Yukawa couplings, and their phases are therefore small. The lengthy expressions in Appendix C can be simplified by expanding these exponents to first order in the phases. Say, the one for the $d$ quark contains the heaviest quark masses in the expression, and the corresponding $CP$ asymmetry is

$$A_{CP} \sim 2J\frac{m_b^2(T)m_c^2(T)}{M_\rho^4(T)} \sim 2J\left(\frac{m_b^2(0)m_c^2(0)}{m_t(0)^4}\right)\left(\frac{m_t(0)^4}{M_\rho^4}\right) \approx J \times 1.2 \times 10^{-7} \times 350 \sim 10^{-9}. \tag{40}$$

*Stage 2:* This corresponds to a top quark mass *large*, $m_t > M_\rho$, making the phase also large, $\phi_t \gg 1$. Since it means a rapidly oscillating exponent, we assume that

$$e^{\pm i\phi_t} \approx 0$$

and drop all factors with a top quark phase. If one starts from a light quark $U0 = u$, the resulting expression contains the mass differences with the heaviest remaining masses of $b$, $c$ quarks, namely,

$$2J\frac{(m_b^2 - m_s^2)(m_c^2 - m_u^2)}{M_\rho^4}. \tag{41}$$

It is similar to the expression we had before, but with masses continuing to grow. The numerator grows as the fourth power of VEV $\sim v(T)^4$, and the denominator approximately as its second power due to sphaleron size shrinkage. As a result, the temperature dependence is $\sim v^2(T) \sim (T_{\rm EW} - T)$.

Eventually, the temperature falls to $T = 130$ GeV below which the sphalerons freeze out completely. The prefactor $2J \sim 6 \times 10^{-5}$ and the $CP$ asymmetry (41) is about

$$A_{CP} \sim 0.25 \times 10^{-9} \tag{42}$$

comparable to what one gets by the end of stage 1.

Some remarks are now in order here. Note that if one starts with the first generation $u$ quark, the intermediate ones kept are $b$ and $c$, of the third and second generations. So, as required, all three generations are involved. Yet this does not mean that *all six quark flavors* need to be

involved: in particular, the answer $\Delta P_u$ (in Appendix D) contains a factor $(m_b^2 - m_s^2)$ but not $(m_d^2 - m_s^2)$, as there is no $d$ quark anywhere. Thus there is no $m_s^2$ in our answer. The situation is exactly the same as in the exclusive $b$ decays as we discussed earlier. Only the masses of the quarks explicitly involved in the process, not all six mass differences, need to be present. The full Jarlskog mass factor is not required in exclusive reactions.

So far we considered single quark loops, separate for each of six quark species. Two CKM matrices were put on its outgoing line, and two more into its line of the conjugated amplitude. However, sphaleron explosions create nine quarks simultaneously. [The ones that depend on $SU(2)$ orientation can, e.g., be $u$, $c$, $t$ quarks of three colors each.] Intermediate states induced by CKM can interfere with those on other quark lines, with some Pauli blocking. There are also QCD and QED-induced final state interactions, which are $T$-odd but flavor dependent. A full scale calculation of a complete nine-particle determinant is at the moment not performed.

Let us give an example of the partial cancellation we have in mind. The $CP$ violation for the $d$ quark, $\Delta P_d$ (in Appendix D), has the same magnitude of the $CP$ violation (41) but has *the opposite sign*. Therefore, in the symmetric phase at $T > T_{\rm EW}$, when orientation of the sphaleron zero mode in the $SU(2)$ group space is spherically symmetric, one may worry about cancellation of the $CP$ violations, between contributions of sphalerons that produce more $u$ or more $d$ quarks. Such cancellations, similar to what is seen in leading order effective Lagrangians, are expected to happen only partially when higher order effects (e.g., including electromagnetic interactions) are taken into account. As the $SU(2)$ symmetry gets broken at $T < T_{\rm EW}$ (the phase we discuss), there is no longer any symmetry between up and down weak isospin orientations. The specific Lagrangian for quark interaction with the $Z$ field takes the well-known form

$$L_{\bar{q}qZ} = -\frac{g}{2\cos(\theta_W)} \sum_i \bar{q}_i Z_\mu \gamma^\mu (g_V^i - g_A^i \gamma^5) q_i \quad (43)$$

in which vector and axial constants are different for up and down quarks:

$$g_V^i = t(i) - 2Q_i \sin^2(\theta_W), \qquad g_A^i = t(i),$$

where $t(\pm) = \pm 1/2$ is a weak isospin and $Q_i = (2/3, -1/3)$ are quark electric charges. Therefore the $u$ and $d$ $CP$-violating terms do *not* cancel each other. Since $Q_u - Q_d = +1$ and the sine of the Weinberg angle $\sin(\theta_W) \approx \frac{1}{2}$ are both of order 1, the effective $CP$ violation in the sphaleron explosion remains of order $10^{-9}$.

Completing this section, let us recapitulate the assumptions made and provide additional comments on further steps of this program: (1) we used the sphaleron size $\rho$ as a placeholder for the distance between points at which the fields appear. In the real calculation, coordinates should be integrated over with projections to currents in an actual Feynman diagram defined on top of the fermionic zero mode of the sphaleron explosion; (2) we eliminated the term with the largest phase, that with the top quark mass, assuming that the oscillating term leads to the cancellation of all terms and zero answer. This contribution can be studied further; (3) we put all CKM matrices on a single line of particular flavor and pick up the largest contribution. A complete calculation with nine lines and the final state QED/QCD interactions is yet to be done.

Note that we are discussing the cosmological time near the phase transition; the quark masses under consideration are not fixed but vary in time, from zero to their physical values in the broken phase, due to a changing Higgs VEV $v$. Suppose we consider the situation in which the largest phase is of order one. We estimate this to happen when

$$m_t(T) \sim \sqrt{E/\rho} \sim M_\rho. \quad (44)$$

This delicate estimate is straightforward in logic but relies on a key assumption, namely, that the energy of the outgoing quark is larger than $E \sim M_{\rm KW}$. Naively, it cannot be smaller for free quarks in the electroweak plasma, as their interaction with the gluons makes their energy of order $M_{\rm KW}$ even at zero momentum. Yet this assumption can be amended by the fact that the outgoing quarks are *not* free. They are still in the sphaleron field where it is worth recalling that they satisfy

$$(-D^2 + g^2 G_{\mu\nu}\sigma^{\mu\nu})\psi_\lambda = \lambda^2 \psi_\lambda, \quad (45)$$

which contains not only the momentum squared, but also the $g^2A^2$, $g^2G_{\mu\nu}$ term. For a sphaleron, the latter is about $\sim 10/\rho^2$, with the sign depending on the location. Therefore, the eigenvalue spectrum does not start at $\lambda > M_{\rm KW}$ sharply, but extends to smaller values. Indeed, the quarks produced are pulled from the lower continuum, or the Dirac sea.The numerical value estimated above contains $1/\lambda^4$, and thus the result depends on the tail of the spectral density at smaller $\lambda$.

## VI. BARYOGENESIS

### A. Sphaleron transitions out of equilibrium

Before we discuss freeze-out of the sphaleron transitions, it is instructive to recall an analogous case of freeze-out of the "little bang" in heavy ion collisions. A good example is the production of antinucleons $\bar{N}$. In the 1990s the cascade codes predicted a small yield of $\bar{N}$, based on the fact that on average many baryons surround an antinucleon. Since the annihilation cross section $\sigma_{N\bar{N}}$ is large, the antinucleon lifetime $\tau \sim 1/(n_N \sigma_{N\bar{N}} \langle v \rangle)$ must be quite short. However, the data showed otherwise, with a number of produced

antinucleons much larger than predicted by the numerical codes. The explanation was given in [34]. The annihilation creates multipion final states with $N_\pi \sim 6$, and the inverse reaction $N_\pi \to N\bar{N}$ was ignored because of certain prejudice, that the multiparticle collision has a negligible rate. Explicit calculations showed otherwise, in agreement with the detailed balance in thermal equilibrium.

This equilibrium is violated only after the so-called *chemical freeze-out*, when the rate $\Gamma_{\rm inelastic}$ of the inelastic reactions changing $N_\pi$ and $N_N$ gets *smaller* than the expansion rate of the fireball $H = \partial_\mu u^\mu$ (the Hubble of the little bang). While the particle numbers become time independent, the thermal state of the expanding fireball is described via time-dependent chemical potentials, $\mu_\pi(t)$ and $\mu_N(t)$. The annihilation channel contains the fugacity factor $\exp(-2\mu_N/T)$, while the inverse reaction channel contains the fugacity $\exp(-N_\pi\mu_\pi/T)$. Since

$$N_\pi\mu_\pi > 2\mu_N, \tag{46}$$

the inverse production process gets more suppressed than the direct annihilation process. Only then does the antibaryon population start to be somewhat depleted.

We now return to Sakharov's conditions for BAU, the deviation from thermal equilibrium. The sphaleron transitions basically consist of two different stages. The first is a complicated diffusion of the gauge fields *moving uphill* (say, from $N_{CS} = 0$ to $\frac{1}{2}$) by thermal fluctuations, driving the fields to the sphaleron configuration at $N_{CS} = 1/2$. Fortunately, we do not need to understand it. In equilibrium the sphaleron population is given by the Boltzmann factor $\exp(-E_{\rm sp}/T)$. The second is the sphaleron decay *rolling downhill*, say, from $N_{CS} = \frac{1}{2}$ to 1, as described by the real-time solution of the equations of motion in Appendix C. The process is purely Minkowskian with an amplitude $e^{iS}$ and a real action, hence it has unit probability of realization.

In equilibrium, the principle of a detailed balance requires that the backward reaction with $t \to -t$ has a rate equal to the forward reaction. Contrary to common prejudice, this means that a large number of gauge quanta

$$N_W \sim 1/\alpha_{\rm EW} \gg 1$$

plus 12 fermions (required by the anomaly relation) can combine into a coherent field configuration. According to Einstein's fluctuation-dissipation relation, random thermal fluctuations driving the system uphill exactly compensate the number of sphalerons rolling downhill. As Sakharov argued, the presence of $CP$ and thus $T$ violation in the matrix element of the process does not matter, since it is the kinetic prefactors that cancel each other. The thermal occupation factors, Sakharov argued, depend only on masses and/or energies, which are $CP$ invariant.

However, since the Universe is expanding and cools below $T_{\rm EW}$, the Higgs VEV $v(T)$ is growing. The height of the topological mountains is growing with it. Uphill transitions with rates smaller than the Hubble rate $H \sim 1/t_{\rm EW}$ no longer happen. The remaining configurations on the sphaleron path just roll down. They are out of equilibrium, as they are not replaced by the upward-going fluctuations anymore. So, their decay fixes a "time arrow," a condition in which the $CP$-complex nature of the amplitude can affect probabilities.

Admittedly, in this work we have not addressed the dynamics of the freeze-out quantitatively. Perhaps one can do so using the Langevin equation. It may also be possible for lattice real-time studies to model a slow Universe expansion. We can only argue at this point that the approach assuming instantaneous transition from the equilibrium occupations to noninteracting states works quite well in heavy ion collisions, where it accurately predicts the yield ratios for many particle species.

The sphaleron decays get frozen when their rate

$$\exp(-B_{\rm sph}\rho v^2(T)) < 10^{-9}. \tag{47}$$

More specifically, for the large-$\rho$ tail and in the small-$v$ regime near $T_c$, the *inverse* reaction of multiquanta collisions gets frozen first. The argument is based on the observation that the corrections to the sphaleron mass $\Delta E_{\rm sp} = C_{\rm sp}\rho v^2$ is smaller than the modification of the thermal Boltzmann factor of the inverse reaction. The latter can be written as corrections to ultrarelativistic energies of $W$ bosons due to their mass $E_p \approx p + M_W^2/2p$, so the energy in their thermal exponent changes by

$$\Delta E_W = \sum_{i=1}^{N_W} \Delta E_i \approx \frac{N_W}{2p}\left(\frac{M_W(0)}{v(0)/v(T)}\right)^2 \tag{48}$$

after rescaling the $W$ mass. Since $1/p \sim \rho$, this correction is of order $\sim\rho v^2$, but the coefficient $N_W$ is parametrically larger with $N_W \sim 100 = \mathcal{O}(1/\alpha_{\rm EW})$.

### B. Contribution to BAU from out-of-equilibrium sphalerons

Our next step is to calculate the BAU produced by the large-size sphalerons which are out of equilibrium. As detailed above, this requires moving to the freeze-out point, thereby sacrificing nine orders of magnitude in the rate with $F_{\rm freeze-out} \sim 10^{-9}$. This is the regime where the sphalerons decay but are not regenerated. Each electroweak sphaleron changes the baryon number by 3 units, i.e., nine quarks each carrying $\frac{1}{3}$ baryon charge. The baryon number density normalized to the entropy density of matter follows by integrating the rate over the freeze-out time $\Delta t_{\rm FO}$

$$\left(\frac{n_B}{s}\right) = 3A_{CP} \times \left[\frac{\Gamma F_{\text{freeze-out}}}{T_{\text{EW}} s_{\text{EW}}}\right] \times [T_{\text{EW}} t_{\text{EW}}] \times \left[\frac{t_{\text{FO}} - t_{\text{EW}}}{t_{\text{EW}}}\right]. \tag{49}$$

Here $A_{CP}$ is the $CP$ asymmetry, the relative difference between baryon number production and annihilation in a single sphaleron transition. The second factor in square brackets is the out-of-equilibrium sphaleron rate normalized to the total entropy density $s_{\text{EW}}/T_{\text{EW}}^3 = \frac{2\pi^2}{45} 106.75$ (where 106.75 is the number of effective degrees of freedom), which amounts to about $3.2 \times 10^{-18}$. The next factor is the cosmological time in units of the electroweak temperature, which is long and about

$$T_{\text{EW}} t_{\text{EW}} \approx 2.2 \times 10^{15}. \tag{50}$$

The fourth (last) bracket is the available time till freeze-out normalized to the total time. Using Friedmann evolution numbers in Appendix A one gets

$$\frac{t_{\text{FO}} - t_{\text{EW}}}{t_{\text{EW}}} \approx 0.5. \tag{51}$$

Since the entropy in the adiabatic expansion of the Universe is conserved, it is the same at the big bang nucleosynthesis (BBN) time which is mostly in the form of black body photons. The standard Bose gas relation between the entropy density and the photon density is $n_\gamma = 0.1388 s_\gamma$. Substituting all these estimates in (49) gives the baryon-to-photon ratio

$$\left(\frac{n_B}{n_\gamma}\right) = 7.6 \times 10^{-2} A_{CP}. \tag{52}$$

Since the phenomenological value for this ratio, from the BBN fits, is known to be

$$\left(\frac{n_B}{n_\gamma}\right)_{\text{BBN}} = 6 \times 10^{-10}, \tag{53}$$

we conclude that the amount of $CP$ violation required to produce the observed BAU is

$$A_{CP} \approx 0.8 \times 10^{-8}. \tag{54}$$

Our estimates of the $CP$ asymmetry above gave about $A_{CP} \sim 10^{-9}$, an order of magnitude smaller than needed to explain BAU. We think that this discrepancy is still inside the uncertainty of our (quite crude) estimates (54).

## VII. OTHER POTENTIAL OBSERVABLES PRODUCED BY SPHALERON EXPLOSIONS

### A. Production of sound and gravity waves

Most of the studies on the gravity wave generation by the EWPT focus on scenarios based on the first order transition or the "cold" transition, as those usually yield large density fluctuations. To our knowledge, the smooth cross over the transition of the minimal SM has not been considered.

Since the sphaleron explosions give rise to significant deviations from a homogeneous stress tensor of the plasma

$$\Delta T^{\mu\nu} \sim G^{\mu\lambda} G^{\nu}_{\lambda} \sim \frac{1}{g^4 T^4}, \tag{55}$$

one may expect radiation of the gravity waves. The stress tensor from the analytically known sphaleron field (B10) yields long expressions which are not suitable for reproduction here. Instead, we show in Fig. 4 the behavior of $T^{00}(t, r)$ (the energy density) and $T^{33}(t, r)$ (the pressure), which illustrates the time-development of the exploding sphaleron in a spherical shell.

The key point here is to assess the scale dependence of both the sound and the gravity waves triggered by the explosion, which can be expressed using the power-per-volume $dE/d^4x$. Dimensional reasoning shows that the average scale is shifted to smaller sphaleron sizes. The measure for small size sphalerons

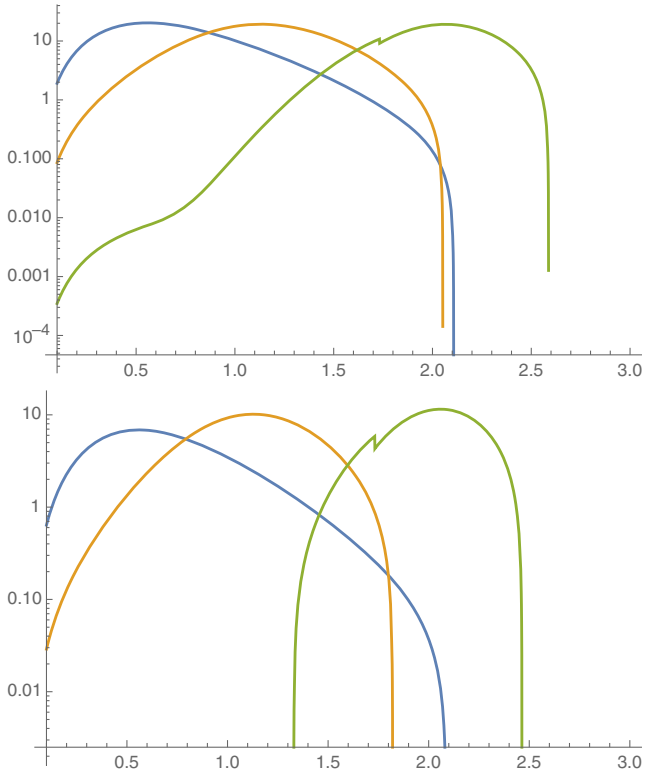


FIG. 4. Components of the stress tensor [times $r^2$, namely, $r^2 T^{00}(t, r)$ upper plot, $r^2 T^{33}(t, r)$ lower plot] as a function of $r$, the distance from the center, at times $t/\rho = 0.1, 1, 2$, left to right.

$$\frac{d\rho}{\rho^5}P(\rho) = d\rho \exp\left(-\frac{3\pi^2}{g^2 T\rho} - 5\log(\rho)\right) \tag{56}$$

is peaked at

$$\rho_* = \frac{3\pi}{20\alpha_{\rm EW}T} \approx \frac{1}{10\ {\rm GeV}}, \tag{57}$$

which is about an order of magnitude smaller than the peak of the distribution (Fig. 1).

Also, for $T > T_c$ we do not expect direct gravitation emission from the sphaleron explosion. In this regime the Higgs VEV vanishes, and nothing breaks the rotational symmetry of the gauge field leading to spherically symmetric sphaleron explosions. As a result, these explosions cannot *directly* generate gravitational waves no matter how violent they are. This is not the case for $T < T_c$ as we discuss below.

There is an *indirect* way to a gravitational signal as discussed in [10]. Spherical sphaleron explosions do excite the underlying medium through hydrodynamical sound waves and vortices. Of course, the medium viscosity will eventually kill them, but since the damping rate scales as $\Gamma \sim \eta k^2$, at small $k$ (large wavelength) this time can be long. A random set of sound sources creates *acoustic turbulence*. Under certain conditions it may turn into the regime of *inverse cascade* and propagate many orders of magnitude, perhaps to the infrared cutoff, the horizon size of the Universe. It is a $2 \to 1$ generic process [10]

$$\text{sound} + \text{sound} \to \text{gravity wave},$$

which operates during the whole lifetime of the sound.

Just after the transition, at $T < T_{\rm EW}$, a nonzero Higgs VEV leads to different masses of various quarks, leptons, and gauge bosons. This "mass separator" split the expanding spherical shell of the explosion into separate regions. Also, a nonzero Weinberg angle (or the nonzero $g'$ coupling of the Higgs to the Abelian $U(1)$ field) produces an elliptic deformation of the sphaleron explosion. It is created by the following part of the action:

$$\Delta S_a = \frac{m_Z^2 - m_W^2}{2}\int d^4x\sqrt{g}g_{\mu\nu}Z^\mu Z^\nu, \tag{58}$$

where the metric is explicitly shown. Writing it as a flat metric plus perturbation $g_{\mu\nu} = \eta_{\mu\nu} + h_{\mu\nu}$ and expanding in $h_{\mu\nu}$ is the standard way to derive the corresponding stress tensor, which is

$$\Delta T_a^{\mu\nu} = \frac{m_Z^2 - m_W^2}{2}\left(-Z^\mu Z^\nu + \frac{\eta^{\mu\nu}}{2}Z^2\right). \tag{59}$$

Here, the prefactor is proportional to $v^2(T)$, nonzero only after EWPT, at $T < T_{\rm EW}$.

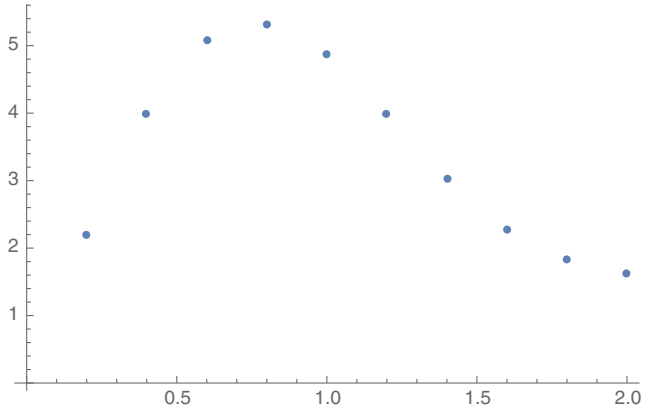


FIG. 5. The dimensionless matrix element $\mathcal{M}/(M_Z^2 - M_W^2)^2$ in (60) versus $k\rho$, for a gravity wave propagating in the one direction with transverse polarization giving $T^{22} - T^{33}$.

The power produced by the gravity wave is proportional to the squared matrix element $|M|^2$ of the Fourier resolved stress tensor by the gravity wave with momentum $\vec{k}$,

$$\mathcal{M}(h,k) = \int d^4x \Delta T^{\mu\nu}(x)h_{\mu\nu}\frac{e^{ik\cdot x}}{r}. \tag{60}$$

We recall that the polarization tensor for the gravity wave $h_{\mu\nu}$ is traceless, and transverse, i.e., nonzero only in the 2D plane normal to $\vec{k}$. For example, for $\vec{k}$ in the one direction, the pertinent contributions in (60) are $T^{22} - T^{33}$ or $T^{23}$ for the respective polarizations.

The main part of the stress tensor gives a vanishing matrix element, as it should, but the asymmetric part of the stress tensor produces gravitational radiation. In Fig. 5 we show the dependence of the gravity wave matrix element as a function of $k\rho$. As expected, it is maximal at $k\rho \sim 1$. We have already evaluated the most important sphaleron size in (57). As a result, the expected gravitational wave momentum should be $k \sim 1/\rho_* \approx 10$–$30$ GeV.

### B. Helical magnetogenesis

The symmetry breaking by the Higgs VEV at $T < T_c$ leads to mass separation of the original non-Abelian field $A_\mu^3$ into a massive $Z_\mu$ and a massless $a_\mu$, related by a rotation involving the Weinberg angle. The expanding outer shell of the sphaleron explosion contains massless photons and near-massless quarks and leptons $u$, $d$, $e$, $\nu$.

The anomaly relation implies that the non-Abelian Chern-Simons number during the explosion defines the chiralities of the light fermions, which can be transferred to the so-called magnetic helicity

$$\int d^3x \boldsymbol{A}\cdot\boldsymbol{B} \sim B^2\xi^4 \sim {\rm const}. \tag{61}$$

The configurations with nonzero (61) are called *helical*. We conclude that the primordial sphaleron explosions may

*seed* the helical clouds of primordial magnetic fields. Since the sphaleron rate is small, $\Gamma/T^4 < 10^{-7}$, these seeds are produced independently from each other, as spherical shells expanding luminally.

The requirement for the inverse cascade effect is chiral unbalance which is at the origin of the chiral magnetic effect (CME). Locally the trapped and comoving light fermions produced by the sphaleron explosion are *chiral*. The time during which chirality is conserved is given by the appropriate fermion masses. For magnetic fields it is the electron mass, which at the sphaleron freeze-out time is

$$m_e(T_{\rm FO}) = m_e \frac{v(T_{\rm FO})}{v(0)} \sim 20 \text{ KeV}. \tag{62}$$

The size growth of the chiral (linked) magnetic cloud is diffusive. For a magnetically driven plasma with a large electric conductivity $\sigma$, a typical magnetic field $\vec{B}$ diffuses as

$$\frac{d\vec{B}}{dt} = D\nabla^2\vec{B} \tag{63}$$

with the diffusion constant $D = 1/(4\pi\sigma) \sim 1/T$. It follows that the magnetic field size grows as

$$R^2(t) = D\Delta t \sim \frac{\Delta t}{T}, \tag{64}$$

where the inverse cascade time $\Delta t$ is limited by the electron mass

$$\Delta t \sim 1/m_e(T_{\rm FO}). \tag{65}$$

As a result, the size of the chiral magnetic cloud is

$$R(\Delta t) \sim \left(\frac{1}{m_e(T_{\rm FO})T}\right)^{\frac{1}{2}} \sim 4 \cdot \text{fm}. \tag{66}$$

We note that this is a few orders of magnitude larger than the UV scale of the problem $1/T \sim 0.001$ fm and far from the IR cutoff of the problem, the horizon at ~2.7 mm.

One of the chief observations is that the magnitude of CKM induced *CP* violation is strongly scale dependent. It increases with the sphaleron size to a maximum, perhaps as large as $\max P_{CP} \sim 10^{-9}$. Therefore, the sphaleron seeded magnetic clouds would start with such an initial asymmetry. Their subsequent evolution goes beyond the scope of this work. However, we expect that during the evolution the left- and right-linked clouds will annihilate. Since helicity in magnetohydrodynamics is conserved, we expect the asymmetry to grow with time till only one chirality remains, as is the case for baryon number.

After the CME is switched off, ordinary magnetohydrodynamical evolution continues to expand the cloud size and to decrease its field strength. This evolution is stopped only when the matter is no longer a plasma, that is, at the recombination era.

## VIII. SUMMARY

The main purpose of this paper is to revive the discussion of the cosmological EWPT, in connection to the generation of the baryon asymmetry and helical magnetic clouds. In contrast to many other works, we have kept our analysis within the minimal SM, using the established fact, from lattice simulations, that the transition is a smooth crossover. The Higgs VEV in it is gradually growing, instead of abruptly jumping, as in the previous first order scenarios.

We have focused on the primordial dynamics of the sphaleron explosions. By now, their overall rate is more or less understood, in both the symmetric and slightly broken phases, from lattice simulations. We have used this knowledge to study the sphaleron size distribution, by constraining the small and large $\rho$-tail distribution to known results.

The small-size end of the sphaleron size distribution, at $\rho \sim 1/(40 \text{ GeV})$ was found to dominate the production of sound waves, as well as direct gravitational radiation. These sound waves may or may not be involved in the inverse acoustic cascade, advocated in [10]. However, if they do, long wavelength sounds would reach the horizon at the time, and then be converted to gravity waves, in a frequency range accessible by eLISA.

In a specific time range between the transition and sphaleron freeze-out $t \in [t_{\rm EW}, t_{\rm FO}]$, we showed that all three Sakharov conditions are satisfied, so the Standard Model does generate *some* baryon asymmetry. The magnitude depends crucially on the *CP* violation during the sphaleron explosion process.

We started our studies of *CP* violation from straightforward estimates of diagrams containing four *W* (and CKM matrices) with two more *Z* bosons added to get a nonzero result. We used the quark Dirac eigenstates as a generic basis. The results should still be convoluted with a spectral density for the particular background. Because of the various interactions with ambient gluons, the quark Dirac eigenspectrum is mostly located at $\lambda \sim M_{\rm KW}$ (the effective mass generated by the forward scattering off gluons). If so, the resulting *CP* asymmetry is about 10 orders of magnitude smaller than needed for the observed BAU ratio. This is a well-known problem, resulting in a pessimistic view of the whole approach.

However, the so-called "topological stability" comes to the rescue. There are good reasons to believe that the Dirac operator in the background of a sphaleron explosion still possesses a topological zero mode, surviving gluon rescattering. This in turn implies that the only place where the Klimov-Weldon mass matters is in the effective mass term for right-handed quarks, as $M_q^2/M_{\rm KW}$. These (flavor-dependent) mass contributions cause additional phase shifts in the outgoing quark waves during their production

process. Moderately involved calculations of the resulting $CP$ asymmetry set its value at about $\sim 10^{-9}$, suppressed by the Jarlskog combination of CKM phases and the fourth powers of the corresponding quark masses.

Comparing to what is needed to solve the famed BAU problem, it is about an order of magnitude off. We think it is well inside the uncertainties of our crude estimates. Anyway, we have shown that a minimal standard model can generate BAU many orders of magnitude larger than previously expected. Clearly, further scrutiny of this scenario is needed.

Finally, we have shown that like the BAU, $CP$ asymmetry at sphaleron explosions should also be at the origin of helical magnetic fields. The conservation of the (Abelian version) of the Chern-Simons number, magnetic linkage, should then keep it till today, and so potentially observable.

## ACKNOWLEDGMENTS

We are grateful to M. Shaposhnikov who patiently criticized earlier versions of this paper. The work is supported by the U.S. Department of Energy, Office of Science, under Contracts No. DE-FG-88ER40388 and No. DE-SC0012704 (D. K.).

## APPENDIX A: BASICS OF ELECTROWEAK PHASE TRANSITION

The transition temperature for the electroweak symmetry breaking was known from the mean field analysis of the Higgs potential and was further detailed by lattice studies in [15]. It is a crossover transition at

$$T_{\rm EW} = (159 \pm 1)\ {\rm GeV}. \tag{A1}$$

The temperature of the Universe today is $T_{\rm now} = 2.73$ K. The ensuing redshift $z$ factor is

$$z_{\rm EW} = \frac{T_{\rm EW}}{T_{\rm now}} \approx 6.8 \times 10^{14}. \tag{A2}$$

During the radiation dominated era, the relation of time to temperature is given by Friedmann relation

$$t = \left(\frac{90}{32\pi^3 N_{\rm DOF}(t)}\right)^{\frac{1}{2}} \frac{M_P}{T^2}. \tag{A3}$$

Inserting the Planck Mass $M_P = 1.2 \times 10^{19}$ GeV, the transition temperature and the effective number of degrees of freedom $N_{\rm DOF} = 106.75$, we find the time after the big bang to be

$$t_{\rm EW} \sim 0.9 \times 10^{-11}\ {\rm s}, \qquad ct_{\rm EW} \approx 2.7\ {\rm mm}. \tag{A4}$$

As explained in the main text, the main phenomena discussed happen near the sphaleron freeze-out time, which, according to Ref. [15], is at $T_{\rm FO} \approx 130$ GeV. The corresponding cosmological time is then

$$t_{\rm FO} \sim 1.36 \times 10^{-11}\ {\rm s}, \qquad ct_{\rm FO} \approx 4 \cdot {\rm mm}. \tag{A5}$$

The Higgs VEV $v(T)$ grows gradually, from zero at the critical $T_{\rm EW}$. It was confirmed by [15] that the squared Higgs VEV grows approximately linearly

$$\frac{v^2(140\ {\rm GeV} < T < T_{\rm EW})}{T^2} \approx 9\left(1 - \frac{T}{T_{\rm EW}}\right). \tag{A6}$$

This scaling is consistent with the naive Landau-Ginzburg treatment of the Higgs potential. The coefficient is also in agreement with the two-loop perturbative calculations. At freeze-out its value is

$$v(T_{\rm FO}) \approx 167\ {\rm GeV}, \tag{A7}$$

approximately $2/3$ of the value in the fully broken phase.

In the symmetric phase $T > T_{\rm EW}$, the normalized sphaleron rate remains constant, which according to [15] is

$$\frac{\Gamma}{T^4} \approx 1.5 \times 10^{-7}, \tag{A8}$$

consistent with the expected magnitude of $18\alpha_{\rm EW}^5$ from perturbative calculations.

If the seeded magnetic field would be simply produced at the electroweak scale $T_{\rm EW}$, and then just grow with the Universe with the redshift factor $z_{\rm EW}$, its resulting spatial scale today would be

$$\xi \sim \frac{z_{\rm EW}}{T_{\rm EW}} = 6.8 \times 10^{14} \times 10^{-18}\ {\rm m} \approx 0.7\ {\rm mm}. \tag{A9}$$

The primary phase of the inverse magnetic cascade can only reach from the microscale of $1/T_{\rm EW} \sim 0.001$ fm to the horizon at that time, $ct_{\rm EW}$, about 13 orders of magnitude away. If that would be the end of the inverse cascade, the correlation length of the magnetic chirality would be

$$\xi \sim \frac{z_{\rm EW}}{1/ct_{\rm EW}} \sim 6.8 \times 10^{14} \times 2.7 \times 10^{-4}\ {\rm m} \approx 10^{12}\ {\rm m}. \tag{A10}$$

This distance may appear large on a human scale, but in units used for intergalactic distances it is tiny $\frac{1}{3} \times 10^{-11}$ Mpc. This scale is also the same as the predicted maximal wavelength of the gravity waves emitted at the electroweak transition today, in the hypothetical inverse acoustic cascade [10].

## APPENDIX B: PURE GAUGE SPHALERONS AND THEIR EXPLOSION

Both static and time-dependent exploding solutions for the pure-gauge sphaleron have been originally discussed by Carter, Ostrovsky, and Shuryak (COS) [8]. Its simpler

derivation, to be used below, has been discussed by Shuryak and Zahed [9]. The construction relies on an *off-center conformal transformation* of the $O(4)$ symmetric Euclidean solution, which is analytically continued to Minkowski spacetime. The focus of the work in [9] was primarily the detailed description of the fermion production.

The original $O(4)$-symmetric solution is given by the following ansatz:

$$gA_\mu^a = \eta_{a\mu\nu}\partial_\nu F(y),$$
$$F(y) = 2\int_0^{\xi(y)} d\xi' f(\xi') \tag{B1}$$

with $\xi = \mathrm{Log}(y^2/\rho^2)$ and $\eta_{a\mu\nu}$ the 't Hooft symbol. Upon substitution of the gauge fields in the gauge Lagrangian one finds the effective action for $f(\xi)$,

$$S_{\mathrm{eff}} = \int d\xi\left[\frac{\dot{f}^2}{2} + 2f^2(1-f)^2\right], \tag{B2}$$

corresponding to the motion of a particle in a double-well potential. In the Euclidean formulation, as written, the effective potential is inverted

$$V_E = -2f^2(1-f)^2, \tag{B3}$$

and the solution going from one maximum to another is the well-known Belavin-Polyakov-Schwarz-Tyupkin (BPST) instanton, a path connecting the two maxima of $V_E$, at $f = 0$, 1. Any other solution of the equation of motion following from $S_{\mathrm{eff}}$ obviously generalizes to a solution of the Yang-Mills equations for $A_\mu^a(x)$ as well. The sphaleron itself is the static solution at the top of the potential between the minima with $f = -1/2$.

The next step is to perform an off-center conformal transformation

$$(x+a)_\mu = \frac{2\rho^2}{(y+a)^2}(y+a)_\mu \tag{B4}$$

with $a_\mu = (0,0,0,\rho)$. It changes the original spherically symmetric solution to a solution of the Yang-Mills equation depending on the new coordinates $x_\mu$, with separate dependences on time $x_4$ and the three-dimensional radius $r = \sqrt{x_1^2 + x_2^2 + x_3^2}$.

The last step is the analytic continuation to Minkowski time $t$, via $x_4 \to it$. The original parameter $\xi$ in terms of these Minkowskian coordinates, which we still call $x_\mu$, has the form

$$\xi = \frac{1}{2}\mathrm{Log}\left(\frac{y^2}{\rho^2}\right) = \frac{1}{2}\mathrm{Log}\left(\frac{(t+i\rho)^2 - r^2}{(t-i\rho)^2 - r^2}\right), \tag{B5}$$

which is pure imaginary. To avoid carrying the extra $i$, we use the real substitution

$$\xi_E \to -i\xi_M = \arctan\left(\frac{2\rho t}{t^2 - r^2 - \rho^2}\right), \tag{B6}$$

and in what follows we will drop the suffix $E$. Switching from imaginary to real $\xi$ corresponds to switching from the Euclidean to the Minkowski spacetime solution. It changes the sign of the acceleration, or the sign of the effective potential $V_M = -V_E$, to that of the normal double-well problem.

The needed solution of the equation of motion has been given in [9]

$$f(\xi) = \frac{1}{2}\left[1 - \sqrt{1+\sqrt{2\epsilon}}\,\mathrm{dn}\left(\sqrt{1+\sqrt{2\epsilon}}(\xi - K), \frac{1}{\sqrt{m}}\right)\right], \tag{B7}$$

where $\mathrm{dn}(z,k)$ is one of the elliptic Jacobi functions, $2\epsilon = E/E_s$, $2m = 1 + 1/\sqrt{2\epsilon}$, and $E = V(f_{\mathrm{in}})$ is the conserved energy of the mechanical system normalized to that of the sphaleron energy $E_s = V(f = 1/2) = 1/8$. Since the start from exactly the maximum takes a divergent time, we will start by *pushing* the sphaleron from nearby the turning point with

$$f(0) = f_{\mathrm{in}} = \frac{1}{2} - \kappa, \qquad f'(0) = 0. \tag{B8}$$

The small displacement $\kappa$ ensures that "rolling downhill" from the maximum takes a finite time and that the half-period $K$—given by an elliptic integral—in the expression is not divergent. In the plots below we will use $\kappa = 0.01$, but the results dependent on its value very weakly.

The solution above describes a particle tumbling periodically between two turning points, and so the expression above defines a periodic function for all $\xi$. However, as it is clear from (B6), for our particular application the only relevant domain is $\xi \in [-\pi/2, \pi/2]$. The solution $f(\xi)$ in it is shown in Fig. 6. Using the first three nonzero terms of its Taylor expansion

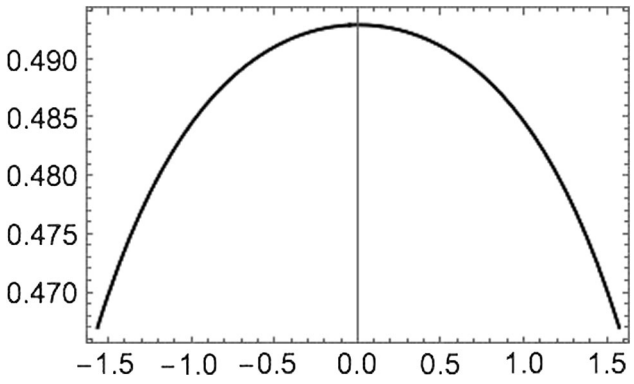


FIG. 6. The function $f(\xi)$ in the needed range of its argument $\xi \in [-\pi/2, \pi/2]$.

$$f \approx 0.49292875 - 0.0070691232\xi^2 - 0.0011773\xi^4 - 0.0000781531899\xi^6, \quad \text{(B9)}$$

we find a parametrization with an accuracy of $10^{-5}$, obviously invisible in the plot and more than enough for our considerations.

The components of the gauge potentials have the form [9]

$$gA_4^a = -f(\xi)\frac{8t\rho x_a}{[(t-i\rho)^2 - r^2][(t+i\rho)^2 - r^2]},$$
$$gA_i^a = 4\rho f(\xi)\frac{\delta_{ai}(t^2 - r^2 + \rho^2) + 2\rho\epsilon_{aij}x_j + 2x_i x_a}{[(t-i\rho)^2 - r^2][(t+i\rho)^2 - r^2]}, \quad \text{(B10)}$$

which are manifestly real. From those potentials we have generated rather lengthy expressions for the electric and magnetic fields, and eventually for the stress tensor and some $CP$-violating operators using *Mathematica*.

Let us only mention that the (static) sphaleron solution is purely magnetic, with $gA_4^a = 0$. The magnetic field squared and summed over all indices give the spherically symmetric simple expression

$$\vec{B}^2 = \frac{96\rho^4}{(\rho^2 + r^2)^4}. \quad \text{(B11)}$$

We note that the specific expressions for pure-gauge sphaleron explosions were compared with numerical real-time simulations [35] where they occur inside the "hot spots" with very good agreement [36]. In the "cold scenario" numerically studied the sphaleron size was not determined by the Higgs VEV in the broken phase, but by the size of the hot spots with the unbroken phase. Unfortunately, a large size tail of the sphaleron distribution on which we focused in this work cannot be studied in similar simulations, as their probability is prohibitively low to reach it statistically.

## APPENDIX C: SPHALERONS DOMINATED BY HIGGS VEV

At $T$ somewhat below $T_{\rm EW}$, when the Higgs VEV $v(T)$ is sufficiently developed, one may return to the original expressions developed by Klinkhamer and Manton [11], modified from $T = 0$ by using appropriate renormalized parameters. With two profile functions, $f(\xi)$, $h(\xi)$ of normalized distance $\xi = gvr$, the sphaleron mass is given by the following integral:

$$M = \frac{4\pi v}{g}\int_0^\infty d\xi\left[4(f')^2 + \frac{8}{\xi^2}f^2(1-f)^2 + \frac{\xi^2}{2}(h')^2 + h^2(1-f)^2 + \frac{\xi^2}{4}\frac{\lambda}{g^2}(h^2-1)^2\right]. \quad \text{(C1)}$$

The mass and size scales include temperature-dependent $v(T)$ which we took from the lattice simulation [15]

$$\frac{v(T)}{T} \approx 3\sqrt{1 - \frac{T}{T_{\rm EW}}}. \quad \text{(C2)}$$

Renormalization of all Standard Model parameters at finite temperatures near $T_{\rm EW}$ has been evaluated, via dimensional reduction, in the fundamental paper [16]. From it, extrapolated to physical Higgs mass in vacuum, we extracted, at $T$ of interest, the following values of the coupling:

$$\frac{\bar{\lambda}_3}{\bar{g}_3^2} \approx 0.22, \qquad \bar{g}_3^2 \approx 0.39, \quad \text{(C3)}$$

and ignore their running in the temperature interval of interest.

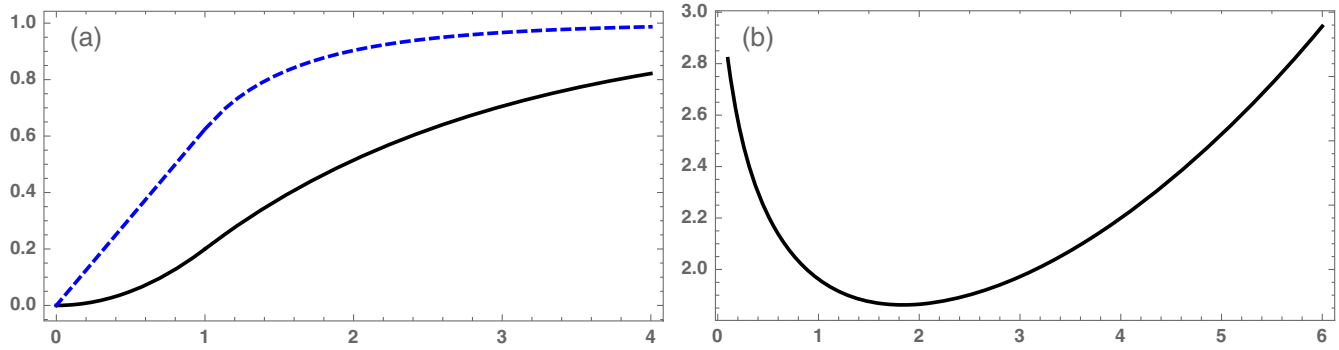


FIG. 7. (a) The profile functions $f(\xi)$, $h(\xi)$ versus $\xi$, for $R = 1$, shown by black solid and blue dashed lines, respectively. (b) Root-mean-square size $\rho(R)$ as a function of parameter $R$.

For calculation we use the so-called ansatz B of [11] with a single parameter $R$

$$f(\xi) = \frac{\xi^2}{R(R+4)}, \quad h(\xi) = \frac{\sigma R + 1}{\sigma R + 2}\frac{\xi}{R} \quad (\xi < R), \tag{C4}$$

$$f(\xi) = 1 - \frac{4}{R+4}e^{(R-\xi)/2}, \quad h(\xi) = 1 - \frac{R}{\sigma R + 2}\frac{1}{\xi}e^{\sigma(R-\xi)} \quad (\xi > R) \tag{C5}$$

with $\sigma = \sqrt{2 \cdot \lambda/g^2}$. These functions are plotted in Fig. 7(a), which, among other features, show their continuity at $\xi = R$. Putting these profiles into the functional (C1), one obtains the sphaleron mass $M(R)$. We also calculated the rms radius of the sphaleron $\rho(R)$, defined by inserting extra $\xi^2$ into the energy density. In the main text we use $M(\rho)$ representation, with $R$ as a parameter.

## APPENDIX D: *CP* VIOLATION AND DIFFERENCES OF QUARK PHASES DURING QUARK PRODUCTION

The multiplication of four CKM matrices by propagators, containing additional phases induced by the quark mass terms in the Dirac operator, leads to the following expressions:

$$\begin{aligned}
\Delta P_t &= 2Je^{-i\phi_c - i\phi_t - i\phi_u}(e^{i\phi_d} - e^{i\phi_s})(e^{i\phi_c} - e^{i\phi_t})(e^{i\phi_c} - e^{i\phi_u})(e^{i\phi_t} - e^{i\phi_u}),\\
\Delta P_c &= 2Je^{-i\phi_c - i\phi_t - i\phi_u}(e^{i\phi_b} - e^{i\phi_d})(e^{i\phi_c} - e^{i\phi_t})(e^{i\phi_c} - e^{i\phi_u})(e^{i\phi_t} - e^{i\phi_u}),\\
\Delta P_u &= 2Je^{-i\phi_c - i\phi_t - i\phi_u}(e^{i\phi_b} - e^{i\phi_s})(e^{i\phi_c} - e^{i\phi_t})(e^{i\phi_c} - e^{i\phi_u})(e^{i\phi_t} - e^{i\phi_u}),\\
\Delta P_b &= 2Je^{-i\phi_c - i\phi_t - i\phi_u}(e^{i\phi_d} - e^{i\phi_s})(e^{i\phi_c} - e^{i\phi_t})(e^{i\phi_c} - e^{i\phi_u})(e^{i\phi_t} - e^{i\phi_u}),\\
\Delta P_s &= 2Je^{-i\phi_c - i\phi_t - i\phi_u}(e^{i\phi_b} - e^{i\phi_d})(e^{i\phi_c} - e^{i\phi_t})(e^{i\phi_c} - e^{i\phi_u})(e^{i\phi_t} - e^{i\phi_u}),\\
\Delta P_d &= 2Je^{-i\phi_c - i\phi_t - i\phi_u}(e^{i\phi_b} - e^{i\phi_s})(e^{i\phi_t} - e^{i\phi_c})(e^{i\phi_c} - e^{i\phi_u})(e^{i\phi_t} - e^{i\phi_u}),
\end{aligned}$$

with

$$J = \cos(\theta_{12})\cos(\theta_{13})^2\cos(\theta_{23})\sin(\theta_{12})\sin(\theta_{13})\sin(\theta_{23})\sin(\delta). \tag{D1}$$

The squared cos is not a misprint. The structure of these expressions is a reminder of the requirement that *CP* violation would vanish if any pair of masses is degenerate. Indeed, in this case we would be able to redefine the CKM matrix and eliminate the complex phase.


[1] E. Witten, Phys. Rev. D **30**, 272 (1984).
[2] K. Kajantie, M. Laine, K. Rummukainen, and M. E. Shaposhnikov, Phys. Rev. Lett. **77**, 2887 (1996).
[3] L. M. Krauss and M. Trodden, Phys. Rev. Lett. **83**, 1502 (1999).
[4] J. Garcia-Bellido, D. Y. Grigoriev, A. Kusenko, and M. E. Shaposhnikov, Phys. Rev. D **60**, 123504 (1999); J. Garcia-Bellido, M. G. Perez, and A. Gonzalez- Arroyo, Phys. Rev. D **67**, 103501 (2003).
[5] A. Tranberg and J. Smit, J. High Energy Phys. 11 (2003) 016; J.-I. Skullerud, J. Smit, and A. Tranberg, J. High Energy Phys. 08 (2003) 045; M. van der Meulen, D. Sexty, J. Smit, and A. Tranberg, J. High Energy Phys. 02 (2006) 029.
[6] M. P. Crichigno, V. V. Flambaum, M. Y. Kuchiev, and E. Shuryak, Phys. Rev. D **82**, 073018 (2010).
[7] A. D. Sakharov, Pis'ma Zh. Eksp. Teor. Fiz. **5**, 32 (1967) [JETP Lett. **5**, 24 (1967)]; Sov. Phys. Usp. **34**, 392 (1991) [Usp. Fiz. Nauk **161**, 61 (1991)].
[8] D. M. Ostrovsky, G. W. Carter, and E. V. Shuryak, Phys. Rev. D **66**, 036004 (2002).
[9] E. Shuryak and I. Zahed, Phys. Rev. D **67**, 014006 (2003).
[10] T. Kalaydzhyan and E. Shuryak, Phys. Rev. D **91**, 083502 (2015).
[11] F. R. Klinkhamer and N. S. Manton, Phys. Rev. D **30**, 2212 (1984).
[12] V. A. Kuzmin, V. A. Rubakov, and M. E. Shaposhnikov, Phys. Lett. **155B**, 36 (1985).

[13] P. B. Arnold, D. Son, and L. G. Yaffe, Phys. Rev. D **55**, 6264 (1997).
[14] U. M. Heller, F. Karsch, and J. Rank, Nucl. Phys. B, Proc. Suppl. **63**, 421 (1998).
[15] M. D'Onofrio, K. Rummukainen, and A. Tranberg, Phys. Rev. Lett. **113**, 141602 (2014).
[16] K. Kajantie, M. Laine, K. Rummukainen, and M. E. Shaposhnikov, Nucl. Phys. **B458**, 90 (1996).
[17] S. Y. Khlebnikov and M. E. Shaposhnikov, Nucl. Phys. **B308**, 885 (1988).
[18] G. D. Moore, Do we understand the Sphaleron rate?, *Strong and Electroweak Matter 2000* (World Scientific, Singapore, 2001), pp. 82–94.
[19] A. M. Polyakov, Phys. Lett. **72B**, 477 (1978).
[20] C. Jarlskog, Phys. Rev. Lett. **55**, 1039 (1985).
[21] M. E. Shaposhnikov, Nucl. Phys. **B287**, 757 (1987).
[22] T. Brauner, O. Taanila, A. Tranberg, and A. Vuorinen, J. High Energy Phys. 11 (2012) 076.
[23] J. Smit, J. High Energy Phys. 09 (2004) 067.
[24] G. R. Farrar and M. E. Shaposhnikov, Phys. Rev. D **50**, 774 (1994).
[25] P. M. Saffin and A. Tranberg, J. High Energy Phys. 02 (2012) 102.
[26] A. Hernandez, T. Konstandin, and M. G. Schmidt, Nucl. Phys. **B812**, 290 (2009).
[27] C. Garcia-Recio and L. L. Salcedo, J. High Energy Phys. 07 (2009) 015.
[28] E. V. Shuryak, Zh. Eksp. Teor. Fiz. **74**, 408 (1978) [Sov. Phys. JETP **47**, 212 (1978)].
[29] M. B. Gavela, P. Hernandez, J. Orlof, and O. Pene, Mod. Phys. Lett. A **09**, 795 (1994).
[30] P. Huet and E. Sather, Phys. Rev. D **51**, 379 (1995).
[31] R. N. Larsen, S. Sharma, and E. Shuryak, Phys. Lett. B **794**, 14 (2019).
[32] G. 't Hooft, Phys. Rev. D **14**, 3432 (1976); **18**, 2199(E) (1978).
[33] Y. Burnier and E. Shuryak, Phys. Rev. D **84**, 073003 (2011).
[34] R. Rapp and E. V. Shuryak, Phys. Rev. Lett. **86**, 2980 (2001).
[35] J. Garcia-Bellido, M. Garcia-Perez, and A. Gonzalez-Arroyo, Phys. Rev. D **69**, 023504 (2004); A. Tranberg and J. Smit, J. High Energy Phys. 11 (2003) 016; J.-I. Skullerud, J. Smit, and A. Tranberg, J. High Energy Phys. 08 (2003) 045.
[36] V. V. Flambaum and E. Shuryak, Phys. Rev. D **82**, 073019 (2010).